California AHMCT Program
University of California at Davis
California Department of Transportation

DYNAMIC MODELING OF WHEELED MOBILE ROBOTS

Demick Boyden
Steven A. Velinsky

AHMCT Research Report
UCD-ARR-93-10-05-01

Interim Report of Contract
IA65Q168-MOU 92-9

October 5, 1993

DYNAMIC MODELING OF WHEELED MOBILE ROBOTS

Interim Report

Demick Boyden

and

Steven A. Velinsky

Department of Mechanical and Aeronautical Engineering

University of California, Davis

October 5, 1993

Advanced Highway Maintenance and Construction Technology Program

DISCLAIMER / DISCLOSURE

"The research reported herein was performed as part of the Advanced Highway Maintenance and Construction Technology Program (AHMCT), within the Department of Mechanical and Aeronautical Engineering at the University of California, Davis and the Division of New Technology and Materials Research at the California Department of Transportation. It is evolutionary and voluntary. It is a cooperative venture of local, state and federal governments and universities."

"The contents of this report reflect the views of the author(s) who is (are) responsible for the facts and the accuracy of the data presented herein. The contents do not necessarily reflect the official views or policies of the STATE OF CALIFORNIA or the FEDERAL HIGHWAY ADMINISTRATION and the UNIVERSITY OF CALIFORNIA. This report does not constitute a standard, specification, or regulation."

ABSTRACT

A significant amount of research is being done and has been published on the subject of wheeled mobile robots (WMR's). A great deal of this work is dedicated toward the development of control strategies for tracking WMR's and for the generation of path planning techniques (mostly for the purposes of collision avoidance). A fundamental part of any research in this area involves some way to track the WMR's position and orientation. Most researchers have used kinematic models to accomplish this task arguing that because of the low speeds, low accelerations, and lightly loaded conditions under which WMR's operate, these kinematic models are valid. However, as we advance to the future of WMR's, dynamic modeling of these vehicles becomes increasingly important as wheeled mobile robots are designed to perform heavy duty work and travel at higher speeds.

This research investigates the importance of dynamic modeling of differentially and conventionally steered wheeled mobile robots. The Tethered Mobile Robot (TMR) designed for the purposes of automated highway crack sealing operations is the vehicle which is modeled and simulated in this work. In this paper, a dynamic model including an accurate tire representation is developed for both differentially and conventionally steered TMR's. In addition to these dynamic models, kinematic and simplified dynamic models are also developed for each of the TMR configurations. The simplified dynamic model utilizes greatly simplified tire representations instead of the complex tire model used by the dynamic model. Through the use of simulation, the limits of validity of each of the models is found for the purposes of determining which model is appropriate for a given application. Additionally, the accuracy of the dead reckoning vehicle tracking process is investigated.

EXECUTIVE SUMMARY

A significant amount of research is being done and has been published on the subject of wheeled mobile robots (WMR's). A great deal of this work is dedicated toward the development of control strategies for tracking WMR's and for the generation of path planning techniques (mostly for the purposes of collision avoidance). A fundamental part of any research in this area involves some way to track the WMR's position and orientation. Most researchers have used kinematic models to accomplish this task arguing that because of the low speeds, low accelerations, and lightly loaded conditions under which WMR's operate, these kinematic models are valid. However, as we advance to the future of WMR's, dynamic modeling of these vehicles becomes increasingly important as wheeled mobile robots are designed to perform heavy duty work and travel at higher speeds. A few researchers have derived and made use of dynamic models for WMR's. However, as these models were derived, the methods for modeling tires were restrictive and potentially inaccurate when considering large, 'working' vehicles and the situations they are designed to encounter.

This research investigates the importance of dynamic modeling of differentially and conventionally steered wheeled mobile robots. The Tethered Mobile Robot (TMR) designed for the purposes of automated highway crack sealing operations is the vehicle which is modeled and simulated in this work. The configurations of general wheeled mobile robots along with the specific differentially steered and conventionally steered tethered mobile robot configurations are introduced. The kinematic equations for both the differentially and conventionally steered TMR's are then derived for the purpose of comparison to the other dynamic models. In a similar manner, the simplest possible dynamic model equations are derived for both the differentially and conventionally steered TMR's. This simple dynamic model uses no tire models to predict the tire forces produced by the tires (actually, a very simple tire model had to be used on the front wheel

of the conventionally steered TMR). The reason for doing this is due to the fact that much of the complication of the dynamic model comes from the use of an accurate tire model, and we wanted to establish when it is necessary to use a complex tire model or when simpler methods may be sufficient.

The Dugoff tire friction model which is used to predict the tire forces in the subsequent dynamic models is then introduced and explained. With the tire model established, the dynamic equations for the differentially steered TMR are derived which incorporate the Dugoff tire representation to provide the tire forces. Simulations are run which compare the dynamic model to the kinematic and simplified dynamic models in order to find the limits of validity of each of the differentially steered WMR models. Additionally, the accuracy of the dead reckoning vehicle tracking method is investigated for differentially steered WMR's when driving wheel speeds are used.

In a similar manner, the dynamic equations for the conventionally steered TMR are derived which incorporate the Dugoff tire representation to provide the tire forces. Simulations are run which compare the dynamic model to the kinematic and simplified dynamic models in order to find the limits of validity of each of the conventionally steered WMR models. Again, the accuracy of the dead reckoning vehicle tracking method is investigated for conventionally steered WMR's.

Finally, conclusions and suggestions are made which explain which model is appropriate for a given application. Furthermore, recommendations for extensions of this work which would provide valuable contributions to this area are described.

Table of Contents

List of Figures

List of Symbols

a = Distance from center of mass to caster wheel pivot.

b = Distance from center of mass to rear axle.

C_{lat} = Lateral traction coefficient.

C_{lng} = Longitudinal traction coefficient.

C_x = Longitudinal tire stiffness.

C_y = Lateral tire stiffness.

d = Distance from center of mass to router.

e = Distance from center of mass to passive linkage connection.

F_N = Normal force on tire.

F_x = Longitudinal tire force (Dugoff).

F_{xd} = Desired longitudinal tire force (Dugoff).

F_{xf} = Front wheel longitudinal force.

F_{xrl} = Left driving wheel longitudinal force.

F_{xrr} = Right driving wheel longitudinal force.

F_{xt} = Longitudinal tire force (not tire specific).

F_y = Lateral tire force (Dugoff).

F_{yd} = Desired lateral tire force (Dugoff).

F_{yf} = Front wheel lateral force.

F_{yrl} = Left driving wheel lateral force.

F_{yrr} = Right driving wheel lateral force.

g = Acceleration of gravity.

G = Center of mass location.

I_Q = Vehicle moment of inertia about point Q about $\hat{k}_2$ (body centered reference frame).

I_t = Wheel, gearbox, and motor rotor moment of inertia as seen at the wheel.

I_x = Vehicle moment of inertia about $\hat{i}_2$ (body centered reference frame).

I_{xz} = Vehicle Product of inertia about $\hat{i}_2$ and $\hat{j}_2$ (body centered reference frame).

I_y = Vehicle moment of inertia about $\hat{j}_2$ (body centered reference frame).

I_z = Vehicle moment of inertia about $\hat{k}_2$ (body centered reference frame).

L_{fx} = Longitudinal force produced by the passive linkage (due to accelerations)

L_{fy} = Lateral force produced by the passive linkage (due to accelerations).

L_t = Torque produced by the friction in the passive linkage joint.

m = mass of vehicle.

N = Torque applied to the wheel.

O = Passive linkage connection location.

P = Router location.

p = Vehicle roll velocity

P_x = Longitudinal router force.

P_y = Lateral router force.

Q = Center point of rear axle.

q = Vehicle pitch velocity.

r = Vehicle yaw velocity.

$\mathbf{R_o}$ = Position vector of the linkage connection point (world coordinate system).

R_t = Tire radius.

S = Longitudinal tire slip.

S_c = Combined longitudinal and lateral tire slip.

T_r = Rear wheel track.

u = Vehicle forward velocity (body centered reference frame).

U = Velocity of vehicle along $\hat{i}_1$ direction (world coordinate system).

v = Vehicle lateral velocity (body centered reference frame).

V = Velocity of vehicle along $\hat{j}_1$ direction (world coordinate system).

$\mathbf{V_f}$ = Front wheel velocity vector.

V_{fx} = Front tire longitudinal linear velocity.

V_{fy} = Front tire lateral linear velocity.

$\mathbf{V_G}$ = Velocity vector of the center of mass (point G).

$\mathbf{V}_l$ = Left wheel linear velocity vector.

V_{ltx} = Left tire longitudinal linear velocity.

V_{lty} = Left tire lateral linear velocity.

$\mathbf{V_o}$ = Velocity vector of the linkage connection point (world coordinate system).

$\mathbf{V}_r$ = Right wheel linear velocity vector.

V_{rtx} = Right tire longitudinal linear velocity.

V_{rty} = Right tire lateral linear velocity.

w = Vertical vehicle velocity (body centered reference frame).

X_1 = Displacement of vehicle along the $\hat{i}_1$ direction (world coordinate system)

Y_1 = Displacement of vehicle along the $\hat{j}_1$ direction (world coordinate system)

Z = Front wheel pivot point.

α_f = Front tire slip angle.

δ = Steered angle.

λ = Ratio of lateral velocity to longitudinal velocity of the tire.

μ = Dynamic coefficient of friction.

μ_d = Desired coefficient of friction.

μ_o = Nominal road/tire interface coefficient of friction.

μ_{res} = Resultant coefficient of friction.

ρ = vector from point Q to center of mass (point G).

ρ_{rr} = Front wheel rolling resistance coefficient.

ω = Wheel angular velocity.

ω_0 = Initial wheel angular velocity.

ψ = Yaw angle.

CHAPTER 1. INTRODUCTION

1-1. Applications of Wheeled Mobile Robots.

Applications for Wheeled Mobile Robots (WMR's) have grown significantly in the last few years and will continue to expand in the future. The potential for the use of these unmanned vehicles to handle inherently hazardous situations or tedious tasks is nearly unlimited. Safety of human life is perhaps the most important advantage for using a WMR in any application.

Wheeled Mobile Robots have been used, in one form or another, to perform janitorial office tasks, to disarm bombs, to clean up hazardous chemical spills, to aid in research, and much more. As the technology is developed, their uses will become widespread and common. WMR's are now being developed for such applications as automated highway transportation, and as is discussed in this paper, automated highway maintenance and repair.

Conceptually developed at the University of California, Davis in conjunction with the California Department of Transportation as part of the Advanced Highway Maintenance and Construction Technology program is the Tethered Mobile Robot (TMR). The TMR is a differentially steered, self-propelled robot which works in close proximity to a support vehicle designed as an integral part of automated highway crack sealing operations. The TMR will house such items as a pavement router and sealant dispenser and will be tethered to the support vehicle by a passive linkage. The passive linkage will serve as a means for delivering supplies and power from the support vehicle to the TMR as well as a means for accurate measurement of the robot's position relative to the support vehicle. A wheeled mobile robot of this configuration has the potential for a wide variety of applications including highway maintenance tasks (pavement crack sealing and painting), toxic waste clean-up, etc.

1-2. Literature Review.

Due to the broad range of potential applications for wheeled mobile robots, a significant amount of research is being done and has been published on the subject. Many researchers have reviewed and investigated different WMR configurations. Most recently, Gentile (1992) reviewed nine different WMR configurations and analyzed the stability and dexterity of each configuration as well as the number of actuators necessary to control and propel the WMR. Many different configurations of WMR's have also been built, including such mobile robots as Newt, the Stanford Cart, Neptune, Rover, and many more. The general configuration of the tethered mobile robot has already been developed and is classified as a differentially steered, conventionally wheeled mobile robot which will be modeled as a three degree of freedom vehicle.

A great deal of the published research is dedicated to developing control strategies for tracking WMR's and for the generation of path planning techniques (mostly for purposes of collision avoidance). A fundamental part of any research in this area involves some way to track the WMR's position and orientation. Most researchers have used kinematic models to accomplish this task, a process called dead reckoning. Dead reckoning is the process of measuring the rotations of the wheels and using rigid body kinematics to determine the WMR's position and orientation. Segovia, Rombaut, Preciado, and Meizel (1991) used a simple 3 degree of freedom kinematic model to predict the position and orientation of a WMR in their study of path generation methods. Alexander and Maddocks (1989) developed the kinematics and inverse kinematics of WMR's for use during low-speed maneuvering. It was assumed in this study that pure rolling takes place until the inertial forces from accelerations saturate the available frictional forces produced by the tires. Using this method however, errors due to wheel slippage and lack of sensitivity to external forces and inertial effects can accumulate and become significant.

A few researchers have derived dynamic models for wheeled mobile robots. Hemami, Mehrabi, and Cheng (1990) formulated the vehicle dynamic equations in a study of new control strategies for tracking WMR's. This study made use of a linear non-dynamic tire model with the assumption that slip angles are less that 5 degrees. It was also assumed that the forward velocity of the vehicle remained constant, so longitudinal tire forces were neglected. Hamdy and Badreddin (1992) derived the dynamic model for a wheeled mobile robot called RAMSIS. Their model accounted only for slip and forces in the longitudinal direction, while side slip was assumed zero and lateral tire forces were neglected. As these dynamic models were derived, the methods for modeling tires are potentially inaccurate when considering large, 'working' vehicles and the situations they are designed to encounter.

1-3. Problem Statement

Most wheeled mobile robots in existence are small and lightweight and operate at low speeds, low accelerations, and under lightly loaded conditions. Because of this, modeling the vehicle dynamics when developing control strategies for WMR's has been considered relatively unimportant (Smith and Starkey, 1991). However, as we advance to the future of WMR's, dynamic modeling of these vehicles becomes increasingly important as wheeled mobile robots are designed to perform heavy duty work and travel at higher speeds (eventually reaching highway speeds). Additionally, a dynamic model must also be accompanied by a reasonably accurate tire model to correctly predict the forces produced by the tires. A dynamic model which utilizes a poor tire representation is potentially inaccurate when operated under conditions which approach the saturation level of the available tire forces.

Most generally, WMR's can be broken up into two categories: differentially steered and conventionally steered. Differentially steered vehicles have two separately controlled driving wheels, and directional control of the vehicle is based on the rotational speeds of the two driving wheels. One or more caster type wheels are used for stability. Conventionally steered vehicles have one or more driving wheels and one or more actively steered wheels. Directional control of the vehicle is based on, of course, steering the steered wheel(s), as in today's automobiles.

The differentially steered vehicle which will be considered in this paper is the Tethered Mobile Robot designed for the purposes of automated highway crack sealing operations. The differential steering will give it the high maneuverability needed to follow crack paths. The TMR is expected to weigh in excess of 2225 N (500 lbs.) and it is being designed to perform heavy duty pavement routing and sealing tasks. Such tasks exert very large external forces on the TMR and will inevitably influence its path and direction. For these reasons, a kinematic model is not sufficiently accurate to predict the

behavior of the TMR. Figure 1-1 depicts an overhead view of the configuration of the differentially steered TMR.

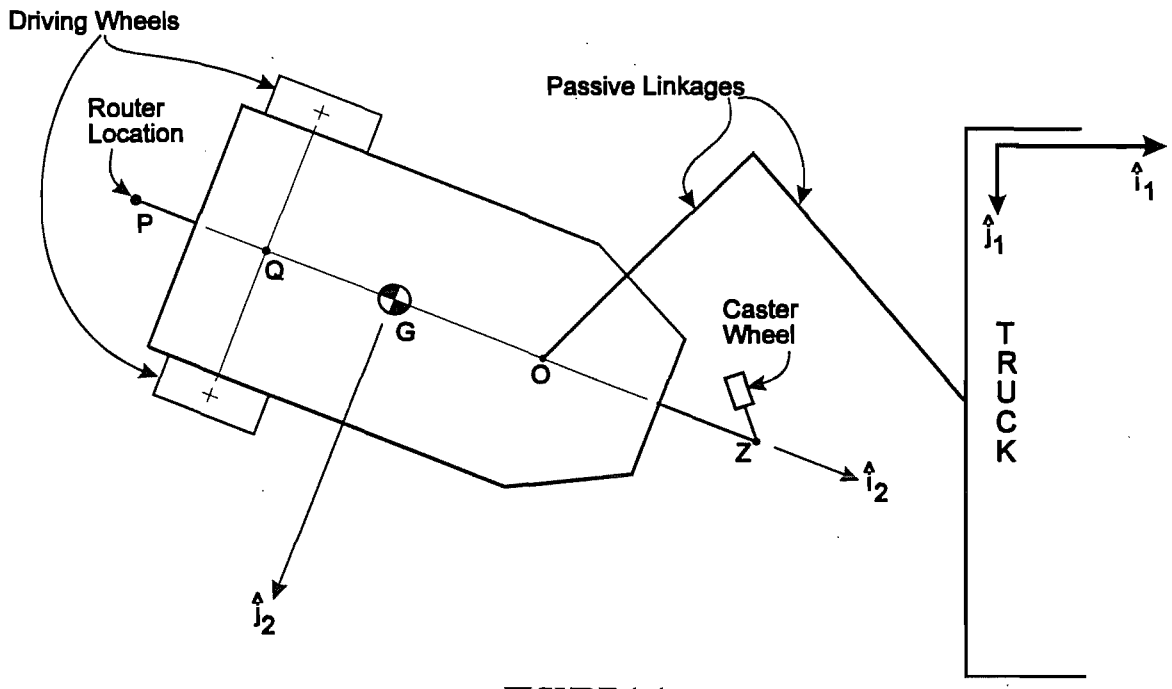

FIGURE 1-1
Overhead view of general configuration of the differentially steered TMR.

In order to investigate the dynamics of conventionally steered WMR's, the differentially steered TMR is easily modified to become a conventionally steered TMR. The front caster wheel is replaced by an actively steered wheel, and the rear wheels are no longer independently controlled. Most all vehicle parameters between the differentially and conventionally steered TMR's are identical.

In this paper, the importance of dynamic modeling is investigated and the limits of validity of kinematic and simplified dynamic models are found. Chapter 2 introduces general wheeled mobile robot configurations along with the differentially steered and conventionally steered tethered mobile robot configurations. Then in Chapter 3, the kinematic equations for both the differentially and conventionally steered TMR's are

derived for comparison to other dynamic models. In a similar manner, the simplest possible dynamic model equations are derived in Chapter 4 for both the differentially and conventionally steered TMR's. In this chapter, no tire models are used to predict the tire forces produced by the tires (actually a very simple tire model had to be used on the front wheel of the conventionally steered TMR). The reason for doing this is due to the fact that much of the complication of the dynamic model comes from the use of an accurate tire model, and we wanted to establish when it is necessary to use a complicated tire model or when a simpler method may be sufficient. Chapter 5 introduces the Dugoff tire friction model which is used to predict the tire forces in the subsequent dynamic models. In Chapter 6 the dynamic equations with the Dugoff tire model for the differentially steered WMR are derived. Simulations are also run in this chapter to compare and find the limits of validity of each of the differentially steered models. Similarly, in Chapter 7 the dynamic equations with the Dugoff tire model for the conventionally steered WMR are derived. Simulations are run which compare and find the limits of validity of each of the conventionally steered models. Finally, Chapter 8 sums up the results and makes recommendations for determining which model is appropriate for a given application.

CHAPTER 2. WHEELED MOBILE ROBOT CONFIGURATIONS

Wheeled mobile robots can be classified into numerous different configurations and types. Campion (1993) classified a large number of WMR configurations into 5 types while Gentile (1992) summarized and compared 9 different WMR architectures. Because of the large number of possible configurations, it is not feasible to try to model and compare every possible type of WMR. However, most all WMR's with conventional wheels can be classified in one of the two following categories: Differentially steered and conventionally steered.

A differentially steered WMR has two separately controlled driving wheels, and directional control of the vehicle is based on the rotational speeds of the two driving wheels. One or more caster type wheels are used for stability.

A conventionally steered WMR has one or more driving wheels and one or more actively steered wheels. If the vehicle has more than one driving wheel, then the driving wheels are normally allowed to turn at different rates, but are supplied with equal torques. This is often accomplished through the use of a single driving motor which transfers power to the driving wheels through a differential. This can also be done with two separate motors which supply equal torques to each of the driving wheels. The directional control of the vehicle is based on the actively steered wheel(s). If multiple steered wheels are used, then it is important that they both steer about the same kinematic center of curvature (Ackermann Steering) or excessive wheel scrub will occur and directional control will be inconsistent. The steered and driving wheels need not be separate, but a single wheel may be both steered and driven.

2-1. The differentially steered wheeled mobile robot.

The differentially steered WMR which will be considered in this paper is the Tethered Mobile Robot designed for the purposes of automated highway crack sealing operations. An overhead view of the differentially steered TMR with all of the forces and moments which are exerted upon it is depicted in Figure 2-1.

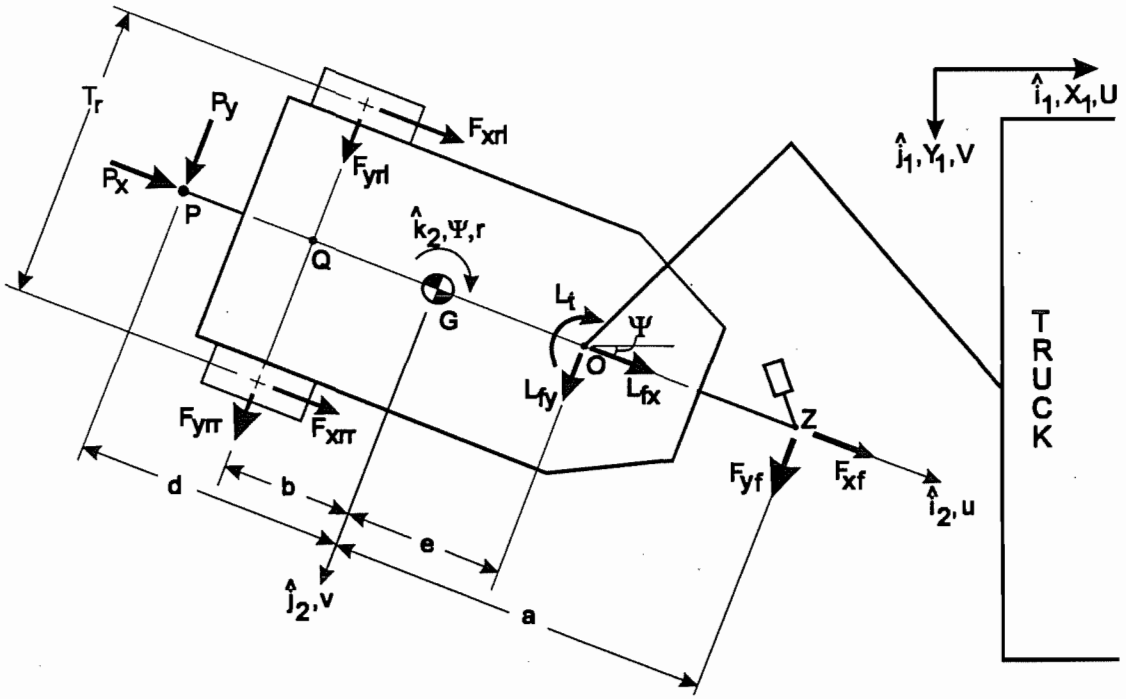

FIGURE 2-1
Differentially Steered Tethered Mobile Robot

Denoted in Figure 2-1 are the following forces and torques:

F_{xrr}, F_{yrr}, F_{xrl}, F_{yrl}: Longitudinal and lateral driving wheel tire forces.

P_x, P_y: Longitudinal and lateral forces produced by the router.

L_{fx}, L_{fy}: Longitudinal and lateral forces produced by the passive linkage (due to accelerations).

L_t: Torque produced by the passive linkage (due to friction in the joint).

F_{xf}, F_{yf}: Longitudinal and lateral rolling resistance produced by the front caster wheel.

2-2. The conventionally steered wheeled mobile robot.

The conventionally steered wheeled mobile robot which will be considered in this paper is nearly identical in configuration to the differentially steered TMR. The front caster wheel is replaced by an actively steered wheel, and the constraint of equally applied torques is imposed on the two rear driving wheels. An overhead view of the conventionally steered TMR with all of the forces and moments which are exerted upon it is depicted in Figure 2-2.

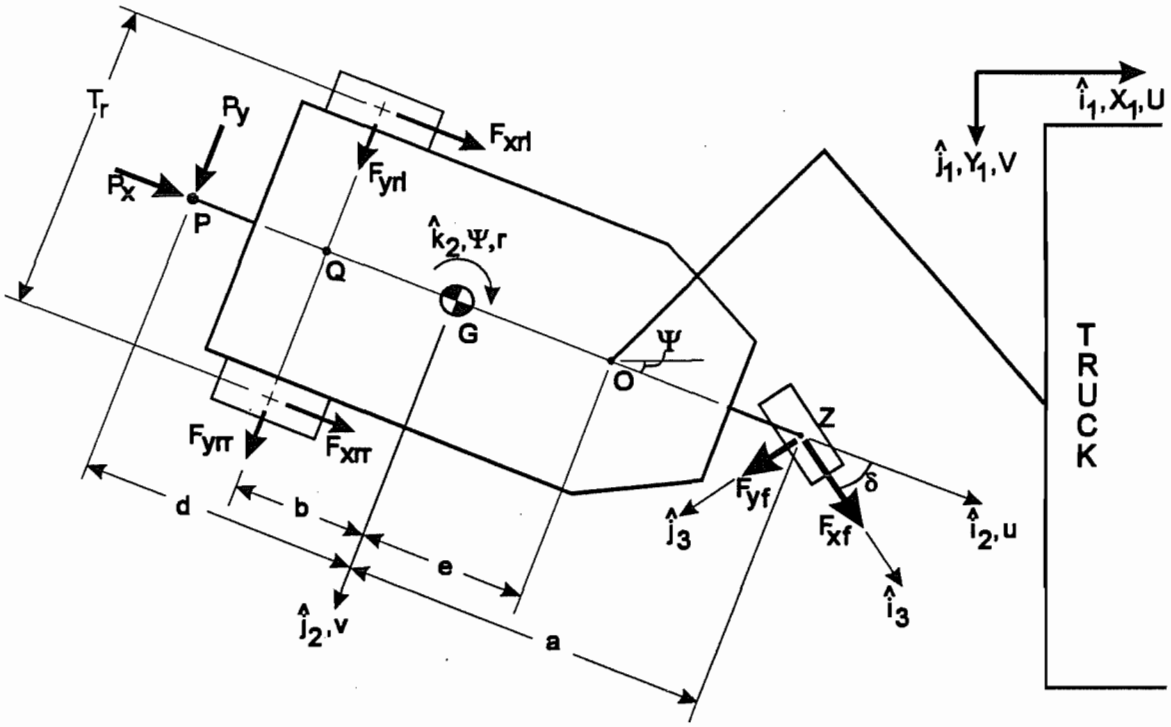

FIGURE 2-2
Conventionally Steered Tethered Mobile Robot

Similar forces as noted in Figure 2-1 are denoted here, with the following exceptions:

F_{xf}, F_{yf}: Longitudinal and lateral front tire forces (WRT tire orientation).

Linkage forces and torques (L_{fx}, L_{fy}, L_t) are not included in this model.

CHAPTER 3. KINEMATICS OF WHEELED MOBILE ROBOTS

Most all models for wheeled mobile robots have used a simple kinematic model to describe the motion of a WMR on a plane. The kinematic model assumes that no tire slippage occurs, so the motion of the WMR can be described using simple rigid body kinematics. In this chapter, the kinematic equations for both differentially steered and conventionally steered wheeled mobile robots are derived.

3-1. Differentially steered wheeled mobile robots.

Using kinematics, it is assumed that no tire slippage occurs, so for the differentially steered TMR, the inputs to the system are left and right wheel angular velocities ω_l and ω_r respectively. With the assumption of no lateral or longitudinal tire slip, the linear velocity of the left wheel, $\mathbf{V}_l$, can be expressed as

$$\mathbf{V}_l = \omega_l R_t \hat{i}_2 \tag{3-1}$$

where R_t denotes the tire radius.

For the cart rigid body we have

$$\begin{aligned} \mathbf{V}_l &= \mathbf{V}_G + r\hat{k}_2 \times (-b\hat{i}_2 - \frac{T_r}{2}\hat{j}_2) \\ &= u\hat{i}_2 + v\hat{j}_2 + r\frac{T_r}{2}\hat{i}_2 - rb\hat{j}_2 \end{aligned} \tag{3-2}$$

where $\mathbf{V}_G$ denotes the velocity vector of the center of mass (point G), r is the vehicle yaw velocity, b is the distance from the rear axle to the center of mass, T_r is the wheel track (center to center distance between the two driving wheels), and u and v are the forward and lateral velocity of the center of mass (point G) of the vehicle respectively.

From (3-1) and (3-2), the following relations for forward and lateral velocity, u and v, are written as

$$u = \omega_l R_t - r\frac{T_r}{2} \tag{3-3}$$

$$v = rb. \tag{3-4}$$

Similarly, for the right wheel linear velocity $\mathbf{V}_r$ we have

$$\mathbf{V}_r = \omega_r R_t \hat{i}_2 \tag{3-5}$$

Examination of rigid body kinematics provides the following expression

$$\begin{aligned} \mathbf{V}_r &= \mathbf{V}_G + r\hat{k}_2 \times (-b\hat{i}_2 + \frac{T_r}{2}\hat{j}_2) \\ &= u\hat{i}_2 + v\hat{j}_2 - r\frac{T_r}{2}\hat{i}_2 - rb\hat{j}_2 \end{aligned} \tag{3-6}$$

and again the forward and lateral velocities can be written as

$$u = \omega_r R_t + r\frac{T_r}{2} \tag{3-7}$$

$v = rb$ *same as (3-4).*

From (3-3) and (3-7), the TMR forward velocity is obtained

$$u = (\omega_r + \omega_l)\frac{R_t}{2}. \tag{3-8}$$

From (3-3) and (3-7) again, the vehicle yaw velocity can be expressed as

$$r = \frac{R_t}{T_r}(\omega_l - \omega_r). \tag{3-9}$$

Substitution of (3-9) into (3-4) yields the following expression for the vehicle lateral velocity

$$v = \frac{R_t b}{T_r}(\omega_l - \omega_r). \tag{3-10}$$

The integral of the yaw velocity is the yaw angle, ψ, which is expressed as

$$\psi = \int r\,dt. \tag{3-11}$$

In the world coordinate system, the velocity of the linkage connection point $\mathbf{V}_o$ of the TMR is

$$\mathbf{V}_o = U\hat{i}_1 + V\hat{j}_1 \tag{3-12}$$

$$U = u\cos(\psi) - v\sin(\psi) - er\sin(\psi) \tag{3-13}$$

$$V = u\sin(\psi) + v\cos(\psi) + er\cos(\psi) \tag{3-14}$$

and the position of the linkage connection point $\mathbf{R}_o$ in the world coordinate system is

$$\mathbf{R}_o = X_1\hat{i}_1 + Y_1\hat{j}_1 \tag{3-15}$$

$$X_1 = \int U\,dt \tag{3-16}$$

$$Y_1 = \int V\,dt. \tag{3-17}$$

3-2. Conventionally steered wheeled mobile robots.

For a conventionally steered WMR, the steered angle δ, and the angular velocity of any one wheel must be specified. For the conventionally steered TMR, the angular velocity of the right rear wheel ω_r will be specified. Relations for the forward and lateral velocities, u and v, using the right rear wheel angular velocity are derived the same as for the differentially steered vehicle and are written as

$$u = \omega_r R_r + r\frac{T_r}{2} \tag{3-7}$$

$$v = rb. \tag{3-4}$$

Using rigid body kinematics, the velocity of the front wheel $\mathbf{V_f}$ can be written as

$$\begin{aligned}\mathbf{V_f} &= \mathbf{V}_G + r\hat{k}_2 \times (a\hat{i}_2) \\ &= u\hat{i}_2 + v\hat{j}_2 + ar\hat{j}_2 \\ &= u\hat{i}_2 + (v + ar)\hat{j}_2.\end{aligned} \tag{3-18}$$

In order to satisfy the no slip conditions at the front wheel, the ratio of the lateral to longitudinal velocity must equal the tangent of the steered angle δ

$$\tan\delta = \frac{v + ar}{u}. \tag{3-19}$$

Substituting in (3-4) for v and rearranging, the yaw velocity can be written as

$$r = \frac{u\tan\delta}{(a+b)} \tag{3-20}$$

and substituting (3-20) into (3-7), the longitudinal velocity can be written in terms of the steered angle instead of the yaw velocity as

$$u = \frac{\omega_r R_t}{1 - \dfrac{T_r \tan\delta}{2(a+b)}}. \tag{3-21}$$

The integral of the yaw velocity is, once again, the yaw angle, which is expressed as

$$\psi = \int r\,dt. \tag{3-11}$$

With the forward, lateral, and yaw velocities, along with the yaw angle, the equations for velocity and position of the conventionally steered TMR in the world coordinate system are identical to those of the differentially steered model.

In the world coordinate system, the velocity of the linkage connection point $\mathbf{V_o}$ of the TMR is

$$\mathbf{V_o} = U\hat{i}_1 + V\hat{j}_1 \tag{3-12}$$

$$U = u\cos(\psi) - v\sin(\psi) - er\sin(\psi) \tag{3-13}$$

$$V = u\sin(\psi) + v\cos(\psi) + er\cos(\psi) \tag{3-14}$$

and the position of the linkage connection point $\mathbf{R_o}$ in the world coordinate system is

$$\mathbf{R_o} = X_1\hat{i}_1 + Y_1\hat{j}_1 \tag{3-15}$$

$$X_1 = \int U\, dt \tag{3-16}$$

$$Y_1 = \int V\, dt. \tag{3-17}$$

CHAPTER 4. SIMPLIFIED DYNAMIC MODELING OF WHEELED MOBILE ROBOTS
(Dynamic modeling with greatly simplified tire representations)

In order to derive the dynamic equations of WMR's, forces must be summed and moments must be taken about some point on the vehicle. This includes forces produced by the tires. Predicting the tire forces is perhaps the most difficult part of the dynamic modeling of a WMR. Although the use of an accurate (and complex) tire model is important, it may not always be necessary. A dynamic model without a tire model is derived here as an example of the simplest possible method of WMR dynamic modeling. Of course there are many simple tire models whose accuracy falls between that of a complex tire model and the example in this chapter with no tire model. This dynamic (without tire) model will be compared to the dynamic (with tire) model to investigate the limits of validity of the no tire dynamic model and the conditions when it is important to use an accurate and sophisticated tire model.

4-1. The body centered frame of reference.

The equations of motion for a wheeled mobile robot are derived in the appendix using the standard vehicle dynamics body centered frame of reference (Gillespie 1992). With respect to the body centered reference frame, the force balance equations for the TMR in the longitudinal, lateral, and vertical directions are expressed as

$$\sum F_x = m(\dot{u} + qw - vr) \tag{4-1}$$

$$\sum F_y = m(\dot{v} + ur - pw) \tag{4-2}$$

$$\sum F_z = m(\dot{w} + pu - qu) \tag{4-3}$$

where q and p are the pitch and roll angular velocities, and w is the vertical bounce velocity.

Also with respect to the body centered reference frame, the moment equations taken about the center of mass (point G) about the longitudinal, lateral, and vertical directions are expressed as

$$\sum M_x = I_x\dot{p} - I_{xz}(\dot{r} + pq) + (I_z - I_y)qr \qquad \textit{(roll)} \qquad (4\text{-}4)$$

$$\sum M_y = I_y\dot{q} + (I_x - I_z)pr + I_{xz}(p^2 - r^2) \qquad \textit{(pitch)} \qquad (4\text{-}5)$$

$$\sum M_z = I_z\dot{r} - I_{xz}(\dot{p} - qr) + (I_y - I_x)pq \qquad \textit{(yaw)} \qquad (4\text{-}6)$$

where I_x, I_y, and I_z are the moments of inertia about the $\hat{i}_2$, $\hat{j}_2$, and $\hat{k}_2$ directions, and I_{xz} is the product of inertia about $\hat{i}_2$ and $\hat{j}_2$.

For a simple 3 degree of freedom planar model which allows only movement in the longitudinal and lateral directions along with angular displacements about the vertical axis (yaw) we have

q = 0 (no pitch),

w = 0 (no bounce),

p = 0 (no roll).

The applicable force and moment equations for the 3 DOF model now become

$$\sum F_x = m(\dot{u} - vr) \qquad (4\text{-}7)$$

$$\sum F_y = m(\dot{v} + ur) \qquad (4\text{-}8)$$

$$\sum M_z = I_z\dot{r}. \qquad (4\text{-}9)$$

4-2. Differentially steered wheeled mobile robots

In the absence of a tire model, a few assumptions and constraints must be made:

- No lateral tire slip ⇒ wheel axle has no lateral velocity.
- Longitudinal tire force is simply some function of the torque applied to the wheel.

Initially it appears that the tire force should simply be the torque applied to the wheel divided by the tire radius. However, upon closer inspection it is apparent that energy to accelerate the wheel, gearbox, and motor rotor must be accounted for (the front caster is assumed to be small and its inertial effects are therefore neglected). Therefore, the tire force produced is proportional to the applied wheel torque minus the amount of torque which is used to accelerate the wheel, gearbox, and rotor. The longitudinal vehicle acceleration including wheel inertia effects is derived here.

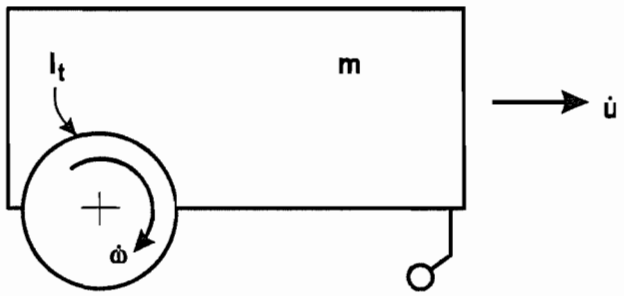

FIGURE 4-1
Side view of differentially steered TMR

Figure 4-1 shows the side view of the differentially steered TMR. Using kinematics, the relation between angular and linear acceleration is obtained

$$\dot{u} = \dot{\omega} R_t . \tag{4-10}$$

The torque applied to the wheel is used in two ways: 1. The linear acceleration of the vehicle and, 2. The angular acceleration of the wheels, gearbox, and rotor: This relation can be expressed as

$$N_{applied} = N_{linear} + N_{angular} \tag{4-11}$$

where $N_{applied}$ is the torque applied to the wheel, N_{linear} is the torque used to linearly accelerate the vehicle, and $N_{angular}$ is the torque used to accelerate the wheels, gearbox, and rotor.

The *linear* torque is simply transformed into a longitudinal tire force F_{xt} at the tire/ground interface and is approximated by

$$F_{xt} = \frac{N_{linear}}{R_t} \tag{4-12}$$

and the *angular* torque accelerates the wheel angular velocity

$$N_{angular} = I_t \dot{\omega} = \frac{I_t \dot{u}}{R_t} \tag{4-13}$$

Combining (4-11), (4-12), and (4-13) yields

$$F_{xt} = \frac{N_{applied} - N_{angular}}{R_t} = \frac{N_{applied} - \dfrac{I_t \dot{u}}{R_t}}{R_t}. \tag{4-14}$$

If a distinction is then made between the right and left rear wheels, (4-14) becomes

$$F_{xrr} = \frac{N_{applied(R)} - \dfrac{I_t \dot{u}_r}{R_t}}{R_t} \qquad \textit{(right wheel)} \tag{4-15}$$

and

$$F_{xrl} = \frac{N_{applied(L)} - \dfrac{I_t \dot{u}_l}{R_t}}{R_t} \qquad \textit{(left wheel).} \tag{4-16}$$

where $\dot{u}_r$ and $\dot{u}_l$ are the longitudinal accelerations of the right and left wheel hubs. Using rigid body kinematics, expressions for these accelerations can be written as

$$\dot{u}_r = \dot{u} - \dot{r}\frac{T_r}{2} \tag{4-17}$$

$$\dot{u}_l = \dot{u} + \dot{r}\frac{T_r}{2}. \tag{4-18}$$

Substitution of (4-17) into (4-15) and (4-18) into (4-16) provides the following expressions for the right and left tire forces

$$F_{xrr} = \frac{N_{applied(R)} - \dfrac{I_t(\dot{u} - \dot{r}\frac{T_r}{2})}{R_t}}{R_t} \tag{4-19}$$

$$F_{xrl} = \frac{N_{applied(L)} - \dfrac{I_t(\dot{u} + \dot{r}\frac{T_r}{2})}{R_t}}{R_t}. \tag{4-20}$$

For the differentially steered Tethered Mobile Robot shown in Figure 2-1, the longitudinal forces can easily be summed by inspection yielding

$$\sum F_x = F_{xrr} + F_{xrl} + P_x + L_{fx} + F_{xf} \tag{4-21}$$

and from (4-7) we get

$$m(\dot{u} - vr) = F_{xrr} + F_{xrl} + P_x + L_{fx} + F_{xf}. \tag{4-22}$$

Substituting in for F_{xrr} and F_{xrl} from (4-19) and (4-20) and solving for the forward acceleration $\dot{u}$ yields

$$\dot{u} = \frac{\dfrac{N_{applied(R)} + N_{applied(L)}}{R_t} + P_x + L_{fx} + F_{xf} + mvr}{m + \dfrac{2I_t}{R_t^2}}. \tag{4-23}$$

The sum of the moments about the z direction taken about the center of mass of the vehicle is (equation (4-9))

$$\sum M_z = I_z \dot{r}. \tag{4-9}$$

However, since the lateral tire forces are unknown because a no lateral slip condition is assumed, the sum of moments must be taken about point Q (centerline of the rear axle) instead of about the center of mass of the vehicle (point G). The general moment equation about point Q is

$$\sum \mathbf{M}_Q = I_Q \dot{\mathbf{r}} + \rho \times m\mathbf{a}_Q \tag{4-24}$$

where I_Q is the Moment of inertia about point Q, ρ is the vector from point Q to center of mass (point G), and $\mathbf{a}_Q$ is the vector of acceleration of point Q.

From the parallel axis theorem:

$$I_Q = I_Z + mb^2 \tag{4-25}$$

and the vector from Q to G is

$$\rho = b\hat{i}_2. \tag{4-26}$$

The acceleration of point Q can be broken up into a longitudinal acceleration, $a_{Q_{long}}$, and a lateral acceleration, $a_{Q_{lat}}$, and is written in vector form as

$$\mathbf{a_Q} = a_{Q_{long}}\hat{i}_2 + a_{Q_{lat}}\hat{j}_2. \tag{4-27}$$

The longitudinal acceleration of point Q is simply the vehicle longitudinal acceleration

$$a_{Q_{long}} = \dot{u} \tag{4-28}$$

and the lateral acceleration is strictly centripetal since point Q has no lateral velocity

$$a_{Q_{lat}} = ur. \tag{4-29}$$

The moment equation (4-24) now becomes

$$\sum \mathbf{M}_Q = [(I_Z + mb^2)\dot{r} + mbur]\hat{k}_2. \tag{4-30}$$

Summing the moments about point Q in the $\hat{k}_2$ direction on the differentially steered TMR shown in Figure 2-1 yields:

$$\sum M_Q = \frac{T_r}{2}(F_{xrl} - F_{xrr}) - (d-b)P_y + (e+b)L_{fy} + L_t + (a+b)F_{yf} \tag{4-31}$$

and substituting in once again for F_{xrr} and F_{xrl} and solving for the yaw acceleration yields:

$$\dot{r} = \frac{\frac{T_r}{2}\left(\frac{N_{applied(L)} - N_{applied(R)}}{R_t}\right) - mbur - (d-b)P_y + (e+b)L_{fy} + L_t + (a+b)F_{yf}}{I_z + mb^2 + \frac{T_r^2 I_t}{2R_t^2}}. \tag{4-32}$$

The longitudinal velocity and the yaw velocity are obtained by simply taking the integral with respect to time of the longitudinal acceleration and yaw angular acceleration

$$u = \int \dot{u}\, dt \tag{4-33}$$

$$r = \int \dot{r}\, dt \tag{4-34}$$

and the yaw angle is the integral with respect to time of the yaw velocity

$$\psi = \int r\, dt. \tag{4-35}$$

Since this model is constrained to have no lateral slip at the tire/ground interface, the expression for lateral velocity of the center of mass of the vehicle, v, is simply obtained through kinematic relations

$$v = br. \tag{4-36}$$

With the forward, lateral, and yaw velocities along with the yaw angle, the equations for velocity and position of the TMR in the world coordinate system are identical to those of the kinematic model at the end of Chapter 3:

In the world coordinate system, the velocity of the linkage connection point $\mathbf{V}_o$ of the TMR is

$$\mathbf{V}_o = U\hat{i}_1 + V\hat{j}_1 \tag{3-12}$$

$$U = u\cos(\psi) - v\sin(\psi) - er\sin(\psi) \tag{3-13}$$

$$V = u\sin(\psi) + v\cos(\psi) + er\cos(\psi) \tag{3-14}$$

and the position of the linkage connection point $\mathbf{R}_o$ in the world coordinate system is

$$\mathbf{R}_o = X_1\hat{i}_1 + Y_1\hat{j}_1 \tag{3-15}$$

$$X_1 = \int U\,dt \tag{3-16}$$

$$Y_1 = \int V\,dt. \tag{3-17}$$

4-3. Conventionally steered wheeled mobile robots.

For the conventionally steered wheeled mobile robot, identical conditions to that of the differentially steered TMR are used at the rear wheels (no rear lateral tire slip and longitudinal tire force a function of the applied wheel torque). Any front tire longitudinal force is assumed to be negligible since there is no torque applied to the front wheel. For the differentially steered TMR, the lateral tire forces never needed to be summed and the vehicle moments were taken about a point on the rear axle. For these reasons, the rear lateral tire forces never needed to be found. The same situation applies to the conventionally steered TMR. However, in this case, there is a front steered wheel which provides lateral tire forces. Because this wheel is steered, the front lateral tire force will

enter into the longitudinal force sum equation. Also there is no point from which to sum the moments which will always cause all three of the lateral tire forces to drop out. For this reason, a very simple tire model must be used to predict the lateral tire force produced by the front wheel. The simplest tire model available is the linear non-dynamic tire model, which simply uses a linear relation between the lateral tire force and the slip angle. To make use of this tire model, the slip angle must first be found. The front slip angle α_f is defined as the angle between the velocity vector $\mathbf{V}_f$ and orientation of the front wheel and is shown in Figure 4-2.

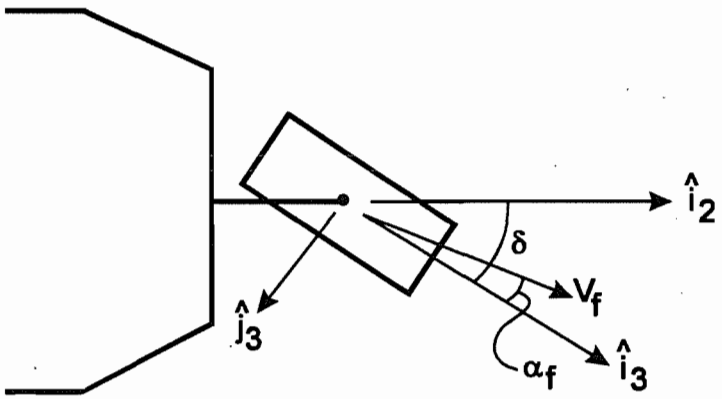

FIGURE 4-2
Steered front wheel defining slip angle.

The front tire velocity is written as

$$\mathbf{V}_f = u\hat{i}_2 + (v + ar)\hat{j}_2 \tag{4-37}$$

and writing the front tire velocity with respect to the tire fixed coordinate system (x_3, y_3, z_3) yields

$$\mathbf{V}_f = [u\cos\delta + (v + ar)\sin\delta]\hat{i}_3 + [(v + ar)\cos\delta - u\sin\delta]\hat{j}_3. \tag{4-38}$$

From its definition, the slip angle can now be written as

$$\alpha_f = \tan^{-1}\left[-\frac{(v+ar)\cos\delta - u\sin\delta}{u\cos\delta + (v+ar)\sin\delta}\right] \tag{4-39}$$

and from the linear non-dynamic tire model, the lateral tire force is the lateral tire stiffness C_{lat} multiplied by the slip angle

$$F_{yf} = C_{lat}\alpha_f . \tag{4-40}$$

The derivation of the rear tire forces is identical to that of the differentially steered vehicle. The right and left rear tire longitudinal forces are therefore expressed as

$$F_{xrr} = \frac{N_{applied(R)} - \frac{I_t(\dot{u} - \dot{r}\frac{T_r}{2})}{R_t}}{R_t} \tag{4-19}$$

$$F_{xrl} = \frac{N_{applied(L)} - \frac{I_t(\dot{u} + \dot{r}\frac{T_r}{2})}{R_t}}{R_t} . \tag{4-20}$$

For the conventionally steered TMR shown in Figure 2-2, the sum of the forces (not including the front longitudinal tire force F_{xf} because it is assumed zero) in the longitudinal direction yields

$$\sum F_x = m(\dot{u} - vr) = F_{xrr} + F_{xrl} - F_{yf}\sin\delta + P_x . \tag{4-41}$$

Substituting in for F_{xrr} and F_{xrl} from (4-19) and (4-20), and solving for the forward acceleration yields

$$\dot{u} = \frac{\frac{N_{applied(R)} + N_{applied(L)}}{R_t} - F_{yf}\sin\delta + P_x + mvr}{m + \frac{2I_t}{R_t^2}}. \quad (4\text{-}42)$$

The moment equation about point Q was derived in section 4-2 and is written as

$$\sum \mathbf{M}_Q = [(I_Z + mb^2)\dot{r} + mbur]\hat{k}_2. \quad (4\text{-}30)$$

Summing the moments about point Q in the $\hat{k}_2$ direction on the conventionally steered TMR shown in Figure 2-2 (also neglecting the longitudinal front tire force F_{xf}) yields

$$\sum M_Q = \frac{T_r}{2}(F_{xrl} - F_{xrr}) + F_{yf}\cos\delta(a+b) - P_y(d-b) \quad (4\text{-}43)$$

and substituting in once again for F_{xrr} and F_{xrl} and solving for the yaw acceleration yields

$$\dot{r} = \frac{\frac{T_r}{2}(\frac{N_{applied(L)} - N_{applied(R)}}{R_t}) - mbur - (d-b)P_y + (a+b)F_{yf}\cos\delta}{I_z + mb^2 + \frac{T_r^2 I_t}{2R_t^2}}. \quad (4\text{-}44)$$

Just as in section 4-2, the longitudinal velocity and the yaw velocity are obtained by simply taking the integral with respect to time of the longitudinal acceleration and yaw angular acceleration

$$u = \int \dot{u}\, dt \quad (4\text{-}33)$$

$$r = \int \dot{r}\, dt \quad (4\text{-}34)$$

and the yaw angle is the integral with respect to time of the yaw velocity

$$\psi = \int r\, dt. \quad (4\text{-}35)$$

Since this model is constrained to have no lateral slip at the rear tire/ground interface, the expression for lateral velocity of the center of mass of the vehicle, v, is simply obtained through kinematic relations

$$v = br. \tag{4-36}$$

With the forward, lateral, and yaw velocities along with the yaw angle, the equations for velocity and position of the TMR in the world coordinate system are identical to those of the kinematic model at the end of Chapter 3:

In the world coordinate system, the velocity of the linkage connection point $\mathbf{V_o}$ of the TMR is

$$\mathbf{V_o} = U\hat{i}_1 + V\hat{j}_1 \tag{3-12}$$

$$U = u\cos(\psi) - v\sin(\psi) - er\sin(\psi) \tag{3-13}$$

$$V = u\sin(\psi) + v\cos(\psi) + er\cos(\psi) \tag{3-14}$$

and the position of the linkage connection point $\mathbf{R_o}$ in the world coordinate system is

$$\mathbf{R_o} = X_1\hat{i}_1 + Y_1\hat{j}_1 \tag{3-15}$$

$$X_1 = \int U\,dt \tag{3-16}$$

$$Y_1 = \int V\,dt. \tag{3-17}$$

CHAPTER 5. THE DUGOFF TIRE FRICTION MODEL

Chapters 6 and 7 will derive the equations for the dynamic modeling of wheeled mobile robots when a tire model which provides longitudinal and lateral tire forces for each tire is used. Before doing this, however, it is necessary to introduce the tire model which will be used as it is an integral part of a dynamic wheeled mobile robot model.

Dugoff's tire friction model, which utilizes the traditional friction circle concept, is used as the basis for calculating tire forces in this paper. Gunter and Sankar (1980) presented a method of simplifying the calculations required when the Dugoff tire model is used for simulation purposes (This method will be referred to as the 'simplified Dugoff tire model'). However, this simplified method is only valid if the vehicle is restricted to forward motion and slip angles of less than 90 degrees. Outside of this range, this simplified method has many inconsistencies associated with it e.g.,

- There are sign errors associated with both longitudinal and lateral predicted tire forces.
- There are no limits placed on slip or on the dynamic coefficient of friction.
- There are pathological cases which are not checked for.
- There are non-holonomic conditions which exist around a vehicle speed of zero.

To correct these inconsistencies the simplified Dugoff model was modified as follows:

- The slip angle has been eliminated. In its place the lateral and longitudinal velocity of the wheel axle are inputs to the subroutine. This eliminates the sign ambiguity associated with the slip angle due to the fact that tangent of the slip angle is a multivalued function in the range of $-\pi$ to π. Certain equations are multiplied by the sign of the lateral or longitudinal velocities to predict the correct values and correct signs for tire forces in any possible vehicle situation.

- Limits have been placed on both the negative and positive maximum values of the longitudinal tire slip. Also the dynamic coefficient of friction has been limited to a minimum value of 70% of the static coefficient of friction. This eliminates the possibility of friction dropping to zero and actually becoming negative.
- Additional pathological cases are checked for to now include all possible situations.
- The non-holonomicity which existed around zero velocity has been removed by checking for an additional pathological case: If the vehicle forward speed is zero, and there is torque applied to the wheel, then the longitudinal force produced by the tire is simply N/R_t (Where N is the applied torque and R_t is the tire radius).

The general procedure for finding the tire forces is outlined below. The equations which correspond to the modified Dugoff tire model are not derived, but simply defined and explained.

First it is necessary to check for pathological cases:

If the tire has no forward velocity V_x, then the longitudinal tire force F_x is

$$F_x = \frac{N}{R_t} \tag{5-1}$$

where N is the torque applied to the wheel and R_t is the tire radius.

If the tire has no forward velocity and no lateral velocity V_y then the lateral tire force F_y is zero

$$F_y = 0. \tag{5-2}$$

If the tire has no forward velocity and a lateral velocity less than 0.03048 m/s (0.1 ft/s) then the lateral tire force is (NOTE: Equation (5-3a) is used if the lateral

velocity V_y is expressed in meters/sec and (5-3b) is used if the lateral velocity is expressed in feet/sec.)

$$F_y = -32.8\mu_o F_n V_y \tag{5-3a}$$

$$F_y = -10\mu_o F_n V_y \tag{5-3b}$$

where μ_o is the nominal coefficient of friction and F_n is the normal load on the tire.

If the tire has no forward velocity and the lateral velocity is greater than 0.03048 m/s (0.1 ft/s) then the lateral tire force is

$$F_y = -\frac{V_y}{|V_y|}\mu_o F_n. \tag{5-4}$$

If none of the previous pathological cases were satisfied, then the tire forces must be solved through the following procedure:

The ratio of the lateral velocity to the longitudinal velocity of the tire λ is a measure of percentage of lateral slip. The absolute value of this ratio is taken because the signs are ignored at this point.

$$\lambda = \left|\frac{V_y}{V_x}\right|. \tag{5-5}$$

The longitudinal tire slip S is the percentage of slip between the tire and the ground. If the wheel angular velocity ω is zero or opposite to the linear longitudinal velocity of the tire, then the longitudinal tire slip = 1. If the wheel angular velocity is not zero and is in the direction of the linear longitudinal velocity of the tire, then the longitudinal tire slip is found with the following expression

$$S = 1 - \frac{R_t \omega}{V_x}. \tag{5-6}$$

Because the equation for longitudinal tire slip is unbounded, a limit must be placed on this value in order to keep other variables which are functions of the longitudinal tire slip within reasonable levels. So, if the calculated longitudinal tire slip is less than -3, then set the longitudinal tire slip to equal -3.

The longitudinal and lateral traction coefficients, C_{lng} and C_{lat}, are given by the following expressions

$$C_{\text{lng}} = 0.001(C_x F_N) \tag{5-7}$$

$$C_{\text{lat}} = 0.001(C_y F_N) \tag{5-8}$$

where C_x and C_y are the longitudinal and lateral tire stiffnesses.

The combined slip S_c is the square root of the sum of squares of the longitudinal slip and the lateral slip

$$S_c = \sqrt{S^2 + \lambda^2} \quad . \tag{5-9}$$

The dynamic coefficient of friction μ is dependent on the amount of slip which is occurring

$$\mu = \mu_o (1 - \varepsilon |V_x| S_c) \tag{5-10}$$

where ε is the dynamic friction reduction factor (0.0034). If the dynamic coefficient of friction is less than 70% of the nominal coefficient of friction, then the dynamic coefficient of friction is limited to 70% of the nominal coefficient of friction.

If the longitudinal slip is 1 (wheels locked), The longitudinal and lateral tire forces are calculated by the following expressions:

$$F_x = \left(-\frac{V_x}{|V_x|} \right) \left[\frac{C_{\text{lng}} \mu F_N}{(C_{\text{lng}}{}^2 + C_{\text{lat}}{}^2 \lambda^2)^{1/2}} \right] \tag{5-11}$$

$$F_y = \left(-\frac{V_y}{|V_y|}\right)\left[\frac{C_{\text{lat}}\mu F_N \lambda}{(C_{\text{lng}}{}^2 + C_{\text{lat}}{}^2\lambda^2)^{1/2}}\right]. \tag{5-12}$$

If the longitudinal slip is not 1, then the desired longitudinal and lateral tire forces, F_{xd} and F_{yd}, must be calculated based on the amount of slip

$$F_{xd} = \left(-\frac{V_x}{|V_x|}\right)\left[\frac{C_{\text{lng}} S}{1-S}\right] \tag{5-13}$$

$$F_{yd} = \left(-\frac{V_y}{|V_y|}\right)\left[\frac{C_{\text{lat}}\lambda}{1-S}\right]. \tag{5-14}$$

Using the desired tire forces, the desired coefficient of friction μ_d can be found

$$\mu_d = \frac{\left(F_{xd}{}^2 + F_{yd}{}^2\right)^{1/2}}{F_N} \tag{5-15}$$

If the desired coefficient of friction is less than 1/2 of the dynamic coefficient of friction, then the desired longitudinal and lateral tire forces are correct. Otherwise, they must be scaled back using a reduced (resultant) coefficient of friction μ_{res}:

$$\mu_{res} = \mu\left(1 - \frac{\mu}{4\mu_d}\right). \tag{5-16}$$

The longitudinal and lateral tire forces can now be predicted using the following equations

$$F_x = F_{xd}\left(\frac{\mu_{res}}{\mu_d}\right) \tag{5-17}$$

$$F_y = F_{yd}\left(\frac{\mu_{res}}{\mu_d}\right). \tag{5-18}$$

This modified Dugoff tire friction model has been thoroughly tested in many different types of maneuvers and situations (including skids and spins). It has been shown to accurately predict tire forces for any situation that a vehicle may encounter.

A flow chart of the procedure is additionally included in Figure 5-1.

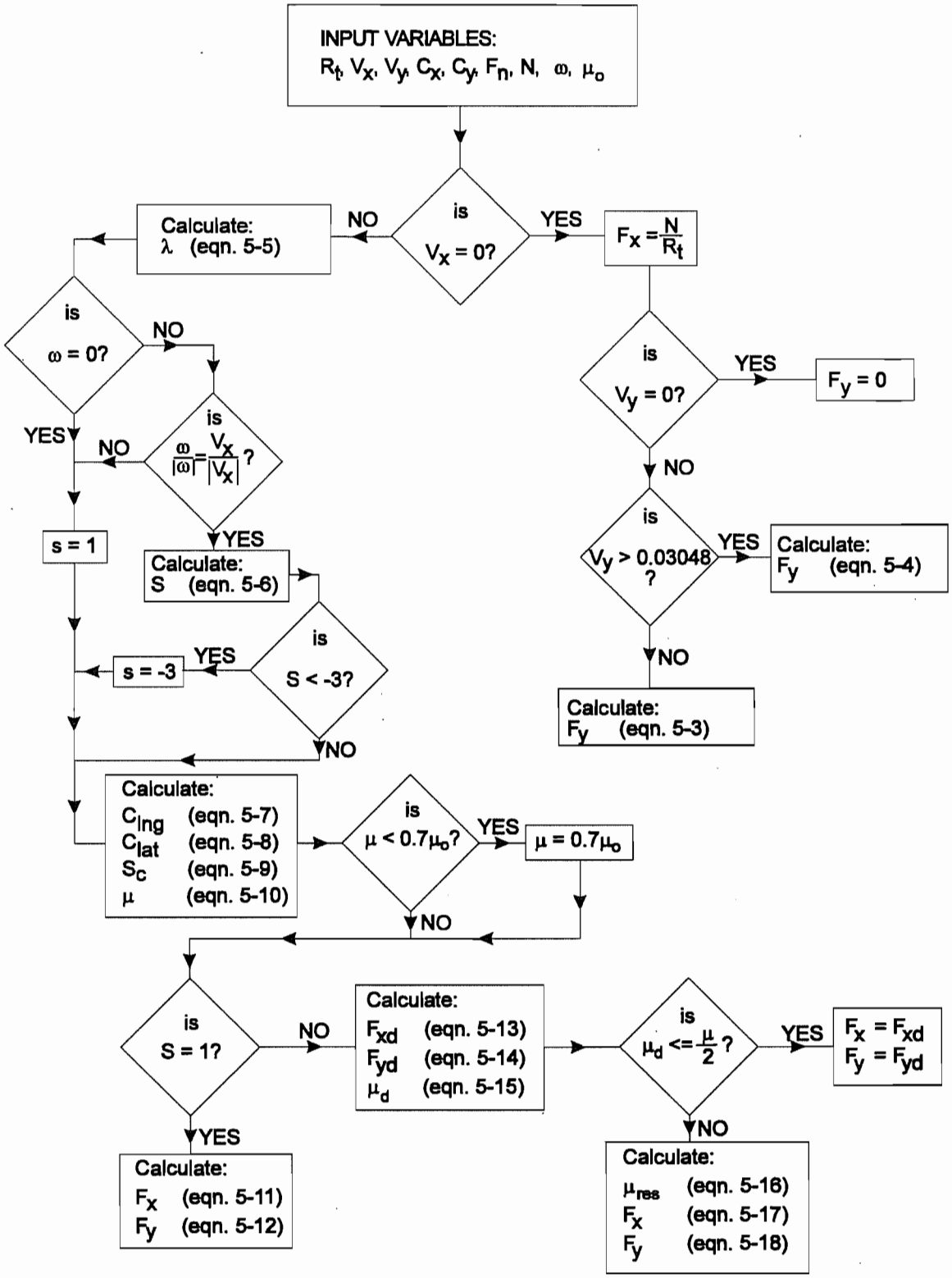

FIGURE 5-1
MODIFIED DUGOFF TIRE FRICTION MODEL FLOW CHART

CHAPTER 6. DYNAMICS OF DIFFERENTIALLY STEERED WHEELED MOBILE ROBOTS

Thus far equations for kinematic and simple dynamic modeling of wheeled mobile robots have been derived. A method for finding tire forces was also presented. In this chapter, the dynamic equations for differentially steered WMR's are derived and the method for finding tire forces presented in Chapter 5 is used to provide the tire forces for the dynamic model. The three differentially steered TMR models are then compared to one another through the use of simulation to find the limits of validity of each model.

6-1. Derivation of Dynamic Equations.

From Chapter 4, the applicable force and moment equations for a 3 DOF model are

$$\sum F_x = m(\dot{u} - vr) \tag{4-7}$$

$$\sum F_y = m(\dot{v} + ur) \tag{4-8}$$

$$\sum M_z = I_z \dot{r}. \tag{4-9}$$

For the differentially steered Tethered Mobile Robot is shown in Figure 2-1, the force and moment equations can easily be summed by inspection yielding

$$\sum F_x = m(\dot{u} - vr) = F_{xrl} + F_{xrr} + P_x + L_{fx} + F_{xf} \tag{6-1}$$

$$\sum F_y = m(\dot{v} + ur) = F_{yrl} + F_{yrr} + P_y + L_{fy} + F_{yf} \tag{6-2}$$

$$\sum M_z = I_z \dot{r} = \frac{T_r}{2}(F_{xrl} - F_{xrr}) - b(F_{yrl} + F_{yrr}) - dP_y + eL_{fy} + L_t + aF_{yf}. \tag{6-3}$$

Solving the three equations for the longitudinal, lateral, and yaw accelerations, $\dot{u}$, $\dot{v}$, and $\dot{r}$ respectively, yields

$$\dot{u} = \frac{F_{xrl} + F_{xrr} + P_x + L_{fx} + F_{xf}}{m} + vr \tag{6-4}$$

$$\dot{v} = \frac{F_{yrl} + F_{yrr} + P_y + L_{fy} + F_{yf}}{m} - ur \tag{6-5}$$

$$\dot{r} = \frac{\frac{T_r}{2}(F_{xrl} - F_{xrr}) - b(F_{yrl} + F_{yrr}) - dP_y + eL_{fy} + L_t + aF_{yf}}{I_z}. \tag{6-6}$$

The three state variables, the longitudinal, lateral, and yaw velocities (u, v, r), are simply the integral of their accelerations

$$u = \int \dot{u}\, dt \quad \textit{(longitudinal velocity)} \tag{6-7}$$

$$v = \int \dot{v}\, dt \quad \textit{(lateral velocity)} \tag{6-8}$$

$$r = \int \dot{r}\, dt \quad \textit{(yaw velocity)}\ . \tag{6-9}$$

The orientation of the vehicle with respect to the world coordinate system (yaw angle) is then determined by taking the integral of the yaw velocity

$$\psi = \int r\, dt. \tag{6-10}$$

With the forward, lateral, and yaw velocities along with the yaw angle, the equations for velocity and position of the TMR in the world coordinate system are identical to those of the kinematic model at the end of Chapter 3:

In the world coordinate system, the velocity of the linkage connection point $\mathbf{V_o}$ of the TMR is

$$\mathbf{V_o} = U\hat{i}_1 + V\hat{j}_1 \tag{3-12}$$

$$U = u\cos(\psi) - v\sin(\psi) - er\sin(\psi) \tag{3-13}$$

$$V = u\sin(\psi) + v\cos(\psi) + er\cos(\psi) \tag{3-14}$$

and the position of the linkage connection point $\mathbf{R}_o$ in the world coordinate system is

$$\mathbf{R}_o = X_1\hat{i}_1 + Y_1\hat{j}_1 \tag{3-15}$$

$$X_1 = \int U\,dt \tag{3-16}$$

$$Y_1 = \int V\,dt. \tag{3-17}$$

TIRE FORCES

It has already been established how the tire forces are found through the use of the Dugoff tire friction model. However, there are a number of parameters which need to be known for the Dugoff model to be able to predict the tire forces:

R_t: Tire radius. (constant)

C_x, C_y: Longitudinal and Lateral tire stiffness parameters. (constant for a set of given conditions; i.e. tire pressure, temperature, etc.)

μ_o: Nominal road/tire interface coefficient of friction. (constant for a given surface)

N: Torque applied to the wheel. Provided as an input to the system.

F_N: Normal Force supported by the wheel. This is assumed to be constant because weight transfer due to acceleration is neglected. The normal force supported by the rear wheels combined is a function of the longitudinal position of the center of mass of the vehicle and is expressed as

$$F_{N(rear)} = mg\frac{a}{a+b}. \tag{6-11}$$

Assuming that the vehicles' center of mass is located along the centerline of the vehicle, the right and left wheel loads are equal and are written as

$$F_{N(left)} = F_{N(right)} = (\frac{mg}{2})\frac{a}{a+b} \tag{6-12}$$

V_x, V_y: Longitudinal and Lateral velocities of the wheel hub. These velocities are found simply by using rigid body kinematics. The right tire linear velocity in the longitudinal and lateral directions are expressed as

$$V_{rtx} = u - r\frac{T_r}{2} \qquad \textit{(longitudinal velocity)} \tag{6-13}$$

$$V_{rty} = v - rb \qquad \textit{(lateral velocity)} \tag{6-14}$$

and the left tire linear velocity in the longitudinal and lateral directions are similarly expressed as

$$V_{ltx} = u + r\frac{T_r}{2} \qquad \textit{(longitudinal velocity)} \tag{6-15}$$

$$V_{lty} = v - rb \qquad \textit{(lateral velocity).} \tag{6-16}$$

ω: Wheel angular velocity. There are two ways of determining the wheel speeds:

1. The wheel speeds are already known because they have been specified as a function of time. This method is used is when comparing the dynamic model to the kinematic model. Since the only way to run a kinematic simulation is to specify the wheel speeds as functions of time, the only way to directly compare the dynamic model to the kinematic model is to also specify the wheel speeds as functions of time. Because the wheel speeds are known at all times throughout the

simulation, slip can be directly calculated and tire forces can be derived from this.

2. In a realistic simulation of a wheeled mobile robot, wheel torques are provided as inputs to the system. However, wheel speeds must be known in order to predict tire forces because tire forces are based on slip - so it is necessary to derive the equations of motion for the wheel. A driving wheel (right or left) is depicted in Figure 6-1.

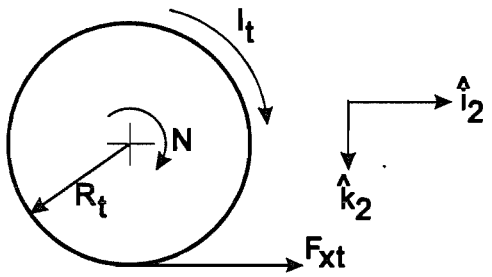

FIGURE 6-1
Right or Left Wheel

As shown in Figure 6-1, N is the applied wheel torque, I_t is the equivalent combined wheel, gearbox, and motor rotor moment of inertia, and F_{xt} is the longitudinal tire force.

Summing the wheel moments yields

$$I_t\dot{\omega} = N - F_{xt}R_t. \tag{6-17}$$

Thus, the wheel angular acceleration $\dot{\omega}$ can be written as

$$\dot{\omega} = \frac{N - F_{xt}R_t}{I_t} \tag{6-18}$$

and wheel speed ω is the integral of the wheel angular acceleration

$$\omega = \int \dot{\omega}\, dt. \tag{6-19}$$

FRONT CASTER ROLLING RESISTANCE

The rolling resistance produced by the front caster wheel is assumed to be opposite to the velocity and proportional to the load on the front wheel (independent of the magnitude of the velocity); i.e., Coulomb friction is assumed in the analysis.

From equation (6-11), the normal load on the front wheel can be expressed as

$$F_{N(front)} = mg\frac{b}{a+b}. \tag{6-20}$$

In order to find the portion of rolling resistance which acts in the longitudinal direction and the portion which acts in the lateral direction, the velocity of the front wheel is needed and can be written in vector form as

$$\mathbf{V_f} = u\hat{i}_2 + (v+ar)\hat{j}_2 \tag{6-21}$$

and the magnitude of this velocity is

$$V_f = \sqrt{u^2 + (v+ar)^2}. \tag{6-22}$$

The portion of rolling resistance which acts in the longitudinal direction is the ratio of the wheel forward velocity to the magnitude of the wheel velocity

$$\frac{u}{\sqrt{u^2 + (v+ar)^2}} \tag{6-23}$$

and the portion which acts in the lateral direction is the ratio of the wheel lateral velocity to the magnitude of the wheel velocity

$$\frac{v+ar}{\sqrt{u^2 + (v+ar)^2}}. \tag{6-24}$$

Accordingly, the rolling resistance produced by the front caster wheel in the longitudinal and lateral directions is expressed as

$$F_{xf} = -\rho_{rr} mg \frac{bu}{(a+b)\sqrt{u^2 + (v+ar)^2}} \qquad \textit{(longitudinal)} \qquad (6\text{-}25)$$

$$F_{yf} = -\rho_{rr} mg \frac{b(v+ar)}{(a+b)\sqrt{u^2 + (v+ar)^2}} \qquad \textit{(lateral)} \qquad (6\text{-}26)$$

where ρ_{rr} is the rolling resistance coefficient.

6-2. SIMULATION AND RESULTS

6-2-1. Comparison of dynamic and kinematic differentially steered models using a wheel speed controlled turning maneuver.

To demonstrate the importance of the dynamic model, it was compared to the kinematic model. To compare these two models, both were run through identical situations to perform a simple maneuver. This maneuver was a simple 90 degree left hand turn similar in nature to a turn that the differentially steered TMR would be expected to perform. Because the kinematic model is used in the comparison, the left and right wheel speeds were the inputs specified as a functions of time. The wheel speed form of the Dynamic model was used accordingly.

The following vehicle parameters and dimensions for this simulation were selected as values characteristic of tethered mobile robot under development (Winters 1992).

TMR mass = 272 kg (18.6 slugs).
Tire radius = 0.3048 m (1.0 ft).
Longitudinal tire stiffness = 40034 N/rad (9000 lbf/rad)
Lateral tire stiffness = 40034 N/rad (9000 lbf/unit slip)
Road/tire interface coefficient of friction = 0.8
Yaw moment of inertia = 407 kg m^2 (300 ft lb sec^2)
Combined wheel, gearbox, and motor rotor moments of inertia = 6.78 kg m^2 (5 ft lb sec^2)

Vehicle dimensions:

a = 0.762 m (2.5 ft).
b = 0.6096 m (2.0 ft).
d = 0.9144 m (3.0 ft).
e = 0.2286 m (0.75 ft).
T_r = 0.9144 m (3.0 ft).

The complete maneuver was accomplished as follows:

- The TMR was initially located at point (0,0) with an orientation of $\phi = 0$ degrees in the world coordinate system with an initial velocity in the $\hat{i}_1$ direction corresponding to the nominal wheel angular velocity (ω_0). Both right and left wheels are spinning at angular velocity ω_0.
- At a certain point in time, the left wheel is decelerated to a stop as a quarter sine wave, held at zero angular velocity for a period of time, and then accelerated back to angular velocity ω_0 (again as a quarter sine wave). The rate that the wheel is decelerated and accelerated and the amount of time at which it is held at zero is dependent on the velocity of the TMR. The right wheel angular velocity is held constant throughout at ω_0. A graph of the left wheel angular velocity is shown in Figure 6-2. This figure is for $\omega_0 = 1$ rad/sec and will vary depending on the value of ω_0 (although the basic shape will remain the same). After the turning maneuver, the TMR is allowed to travel in a straight line for a few moments to

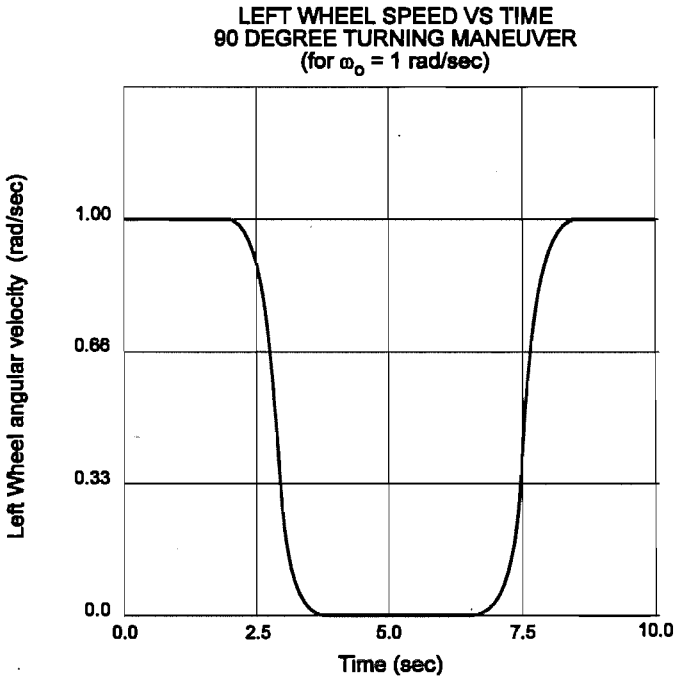

FIGURE 6-2
Left wheel speed as a function of time at $\omega_0 = 1$ rad/sec.

illustrate the difference in predicted paths between the models. The total time simulated varies depending on the speed that the TMR is simulated at (to produce comparable results).

- The maneuver is run at five different vehicle speeds: 0.3048 m/s (1 ft/s), 0.6096 m/s (2 ft/sec), 0.9144 m/s (3 ft/s), 1.524 m/s (5 ft/s), and 3.048 m/s (10 ft/s).

In order to keep the results simple and straightforward to interpret, it is assumed that there are no router forces, no torques or forces from the passive linkages, and no rolling resistance forces from the front caster wheel:

$$P_x = P_y = L_{fx} = P_{fy} = L_t = F_{xf} = F_{yf} = 0.$$

The results from this simulation are quite significant and are shown in Figure 6-3.

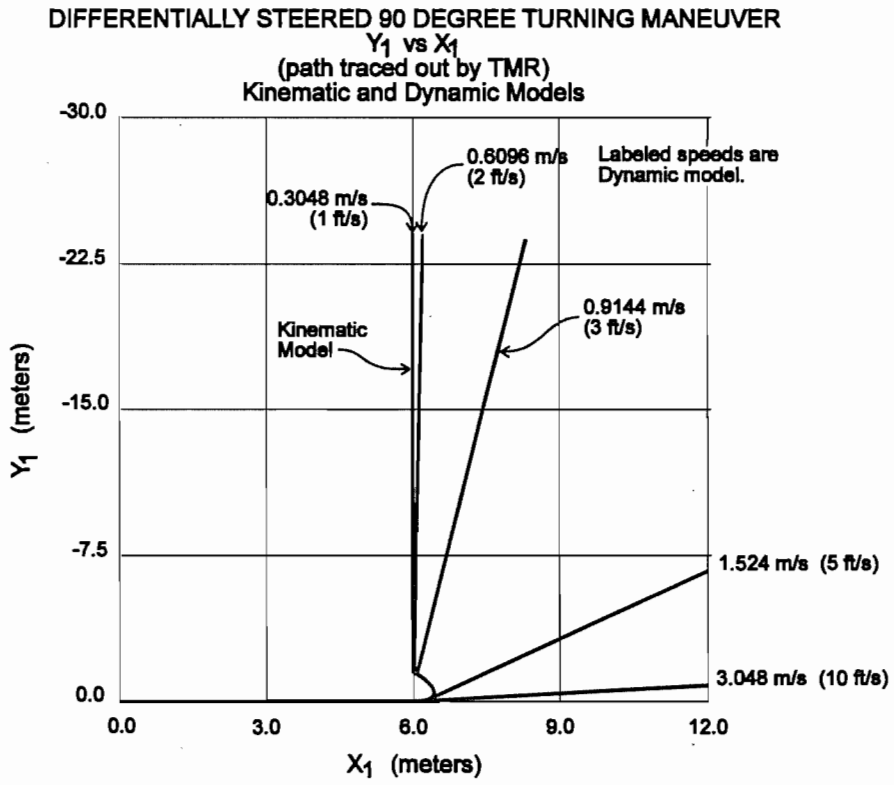

FIGURE 6-3
TMR path trace - 90 Degree turn simulation results.

The predicted path that the vehicle traces out using the kinematic model is independent of initial vehicle speed. As expected, however, the dynamic models' prediction is highly dependent on vehicle speed. At a vehicle speed of about 0.3048 m/sec (1 ft/sec) or less, the predicted results of the dynamic model are identical to that of the kinematic model. At a vehicle speed of 0.6096 m/sec (2 ft/sec) the differences become significant, and at any higher speeds, the differences are drastic. At the higher vehicle speeds, the left tire forces saturate during the maneuver which causes the vehicle to fall short of the designated 90 degree turn. This is, of course, a very sharp turn with a radius of curvature of approximately the rear wheel track of the vehicle (0.9144 m (3 ft)). However, differentially steered vehicles are designed to be highly maneuverable and turns of this sort are expected.

According to these results, a differentially steered wheeled mobile robot simulation using dead reckoning navigation techniques, traveling at a velocity of only 0.9144 m/sec (3 ft/sec) will have a location error of about 2 meters (7 feet), 23 meters (75 feet) after making the turning maneuver.

6-2-2. Comparison of Dead Reckoning method, Dynamic (with tire), and Dynamic (without tire) differentially steered models using a torque controlled turning maneuver.

In the previous simulation, the range of validity of the kinematic model for differentially steered vehicles when used for simulation purposes was shown. The kinematic model can also be used on real vehicles to determine position and orientation by physically measuring wheel speeds - a process called dead reckoning. It is possible to show the range of validity associated with the dead reckoning process by combining the kinematic model with the dynamic model. The kinematic model simply utilizes the wheel speeds which the dynamic model calculates - just as if they had been measured off of the drive wheels of a vehicle. Any differences between the predicted paths of the dead reckoning and dynamic models is entirely due to wheel slippage, and is the same error associated with using the dead reckoning process on a real vehicle. It is important to note that in these simulations, the dead reckoning method is performed using drive wheel speeds. Dead reckoning can also be performed by using wheel speeds measured off of passive wheels, which is more accurate because much of the longitudinal slip error is removed.

For this simulation the applied wheel torques are specified instead of wheel speeds. Using this method, the importance of a tire model can also be determined by comparing the dynamic (with tire) model to a dynamic (without tire) model. A dynamic differentially steered model without a tire model was derived in Section 4-2.

The simulated maneuver for this comparison is again, a left hand turn. However, since the wheel torques are specified, the degree of attempted turn is not predetermined. The left hand turn is accomplished as follows:

- The TMR starts initially at point (0,0) with an orientation of $\psi = 0$ degrees in the world coordinate system with an initial velocity if 0.3048 m/sec (1 ft/sec) in the $\hat{i}_1$ direction. Both the right and left wheels are spinning accordingly. At time t = 0

seconds, equal torques of 27.1 N-m (20 ft-lbf) are applied to the right and left driving wheels.

- At time t = 2 seconds, the torque applied to the left wheel is reversed to -27.1 N-m (-20 ft-lbf). This reversed torque is applied for 2 seconds (until t = 4 seconds), and then resumed to its original 27.1 N-m (20 ft-lbf). The right wheel torque remains constant at 27.1 N-m (20 ft-lbf) throughout. The total time simulated for each situation is identical (6 seconds).

As in the previous simulation, it is assumed that there are no router forces, no torques or forces from the passive linkages, and no rolling resistance forces from the front caster wheel.

For this simulation, the position of the TMR center of mass has been altered for several different comparisons. This will demonstrate the effect that the vehicle inertia has on the different models. Three different center of mass locations were used. Table 6-1 contains the vehicle dimensions for each of the three center of mass locations.

The results of the simulation showing the path traced out by the TMR with the center of mass in each of the three different locations are shown in Figures 6-4 to 6-6. Each figure shows the predicted path for the dynamic (with tire) model, the dynamic (without tire) model, and the dead reckoning method.

Vehicle Dimensions (m [ft])

Position #	Description of C.M. Location	a	b	d	e
1	At linkage connection point O	0.5334 [1.75]	0.8382 [2.75]	1.143 [3.75]	0 [0]
2	At regular C.M. point G	0.762 [2.5]	.06096 [2.0]	0.9144 [3.0]	0.2286 [0.75]
3	On axle point Q	1.3716 [4.5]	0 [0]	0.3048 [1.0]	0.8382 [2.75]

TABLE 6-1
Vehicle dimensions for different center of mass locations

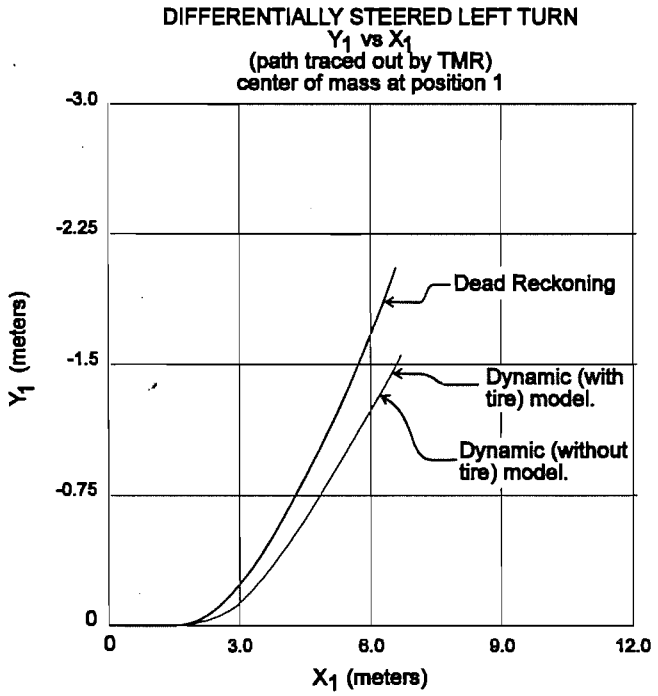

FIGURE 6-4
TMR path trace - Torque controlled turn - C.M. at position # 1

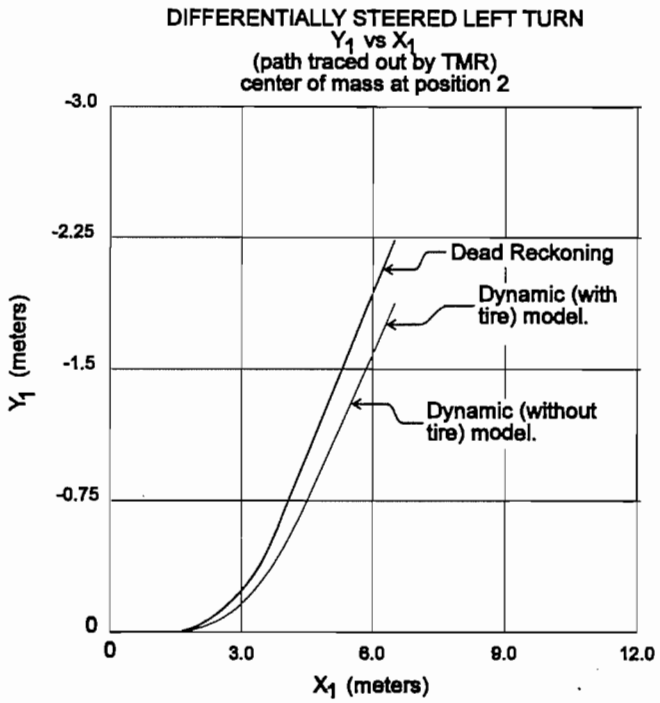

FIGURE 6-5
TMR path trace - Torque controlled turn - C.M. at position #2

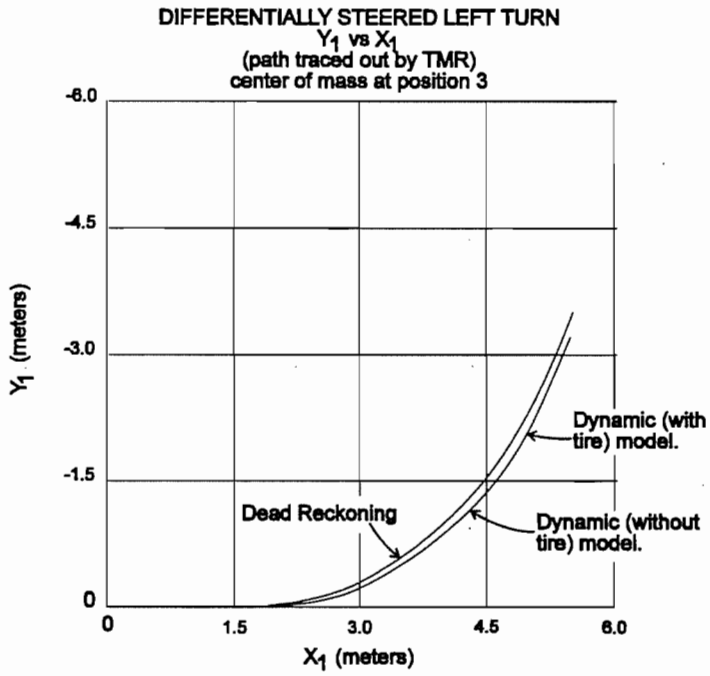

FIGURE 6-6
TMR path trace - Torque controlled turn - C.M in position #3

The results of this torque controlled turn simulation are very significant. Most noticeably, there is no difference between the dynamic (with tire) model and the dynamic (without tire) model in any of the three situations. This must be attributed to the fact that the tire forces are relatively small in these situations.

In comparison of the dynamic models and the dead reckoning method, the greatest differences occur with the center of mass in position #1 and #2. These differences represent the real error associated with tracking a vehicle by measuring the wheel speeds of its driven wheels. In these simulations, the position error is as much as 0.6096 m (2 feet) after the vehicle has only traveled for a total of 6 seconds at relatively low speeds (the maneuver takes place at about 1 m/s (3.5 ft/sec)). This is almost a 10% error.

When the center of mass location is moved to the rear axle, as in position #3, the dead reckoning method's prediction is much more accurate. This is because the inertial effects are decreased because the center of mass is closest to the center of curvature at this position (the kinematic center of curvature lies along the line created by the rear axle).

Perhaps the most interesting results are the tire forces. The longitudinal and lateral left tire forces for the TMR with center of mass in position #2 are shown in Figure 6-7. Only the left tire forces are shown because its forces are the greatest since the left wheel is the one whose applied torque is altered. In general, it is assumed that the dead reckoning technique is a relatively good approximation if the tires are producing forces less than 50% of their limits. For the TMR with C.M. at position #2, the tire limits are about 600 N (135 lbf). From Figure 6-7, the maximum tire forces occur at $t \approx 4$ seconds, at which time the longitudinal and lateral tire forces are about -90 N (-20 lbf) and -45 N (-10 lbf) respectively for a combined tire force of approximately 98 N (22 lbf). This is only 16% of available tire force. Yet there is a 10% error in position after only 6 seconds of travel. This means that the kinematic model with dead reckoning is not necessarily a good approximation even when the tire forces are well within their limits.

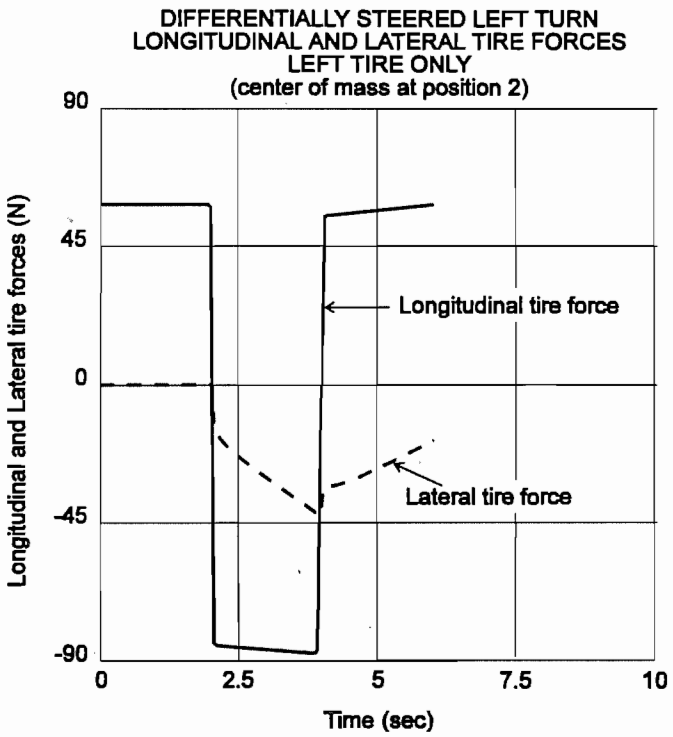

FIGURE 6-7
Left tire forces for torque controlled turn - C.M. at position #2

It is necessary to note, once again, that no external forces were considered in either of these simulations in order to make the results more straightforward to interpret. If external forces had been considered, especially large forces as are expected in the case of the TMR, the paths between the dynamic and kinematic models would have differed to a greater extent. Most noticeably, the paths would deviate more significantly in the case where the center of mass was located on the differentially steered vehicles' rear axle.

6-2-3. Comparison of differentially steered Dynamic (with tire) model to Dynamic (without tire) model using a torque controlled turning maneuver with external forces.

Since the two differentially steered dynamic models produced identical results in the previous section, it is necessary to find the limits of validity of the dynamic (without tire) model. To accomplish this, the same torque controlled turning maneuver is used as in the previous simulation with the following exceptions:

- External longitudinal and lateral router forces of 222 N (50 lbf) are applied to the vehicle throughout the simulation: $P_x = P_y = 222$ N (50 lbf). These router forces comply with router force magnitudes which the TMR is expected to experience.
- Two different values for the magnitude of the torque applied to the wheels are used: 102 N-m (75 ft-lbf) and 204 N-m (150 ft-lbf)
- The position of the center of mass is not varied in any of these simulations. It remains at the regular center of mass point *G* (position #2).

The TMR path trace and left tire forces for the simulation with the 102 N-m torque applied to the wheels are shown in Figures 6-8 and 6-9 respectively. From Figure 6-9, the maximum tire forces occur at $t \approx 4$ seconds, at which time the longitudinal and lateral tire forces are about 333 N (75 lbf) and 500 N (112 lbf) respectively for a combined tire force of approximately 600 N (135 lbf). This shows that the tires are operating right at the limits of their traction abilities during this simulation. Still, the dynamic (without tire) model is relatively accurate, only deviating from the dynamic (with tire) model by about 4%. Of course, over a longer period of time, this error will accumulate and become very significant. However, it is surprising at how accurate the dynamic (without tire) model is considering the fact that the tires are producing forces at their available traction limits.

For demonstration purposes only, the dead reckoning path trace is also shown in Figure 6-8 to show the inaccuracy of this method when the tires operate at their limits.

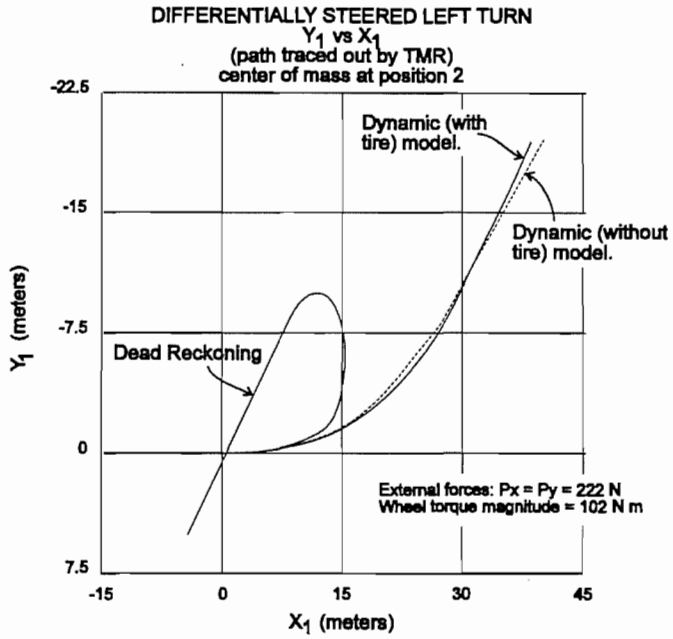

FIGURE 6-8
TMR path trace - Torque controlled turn - 102 N-m (75 ft-lbf)

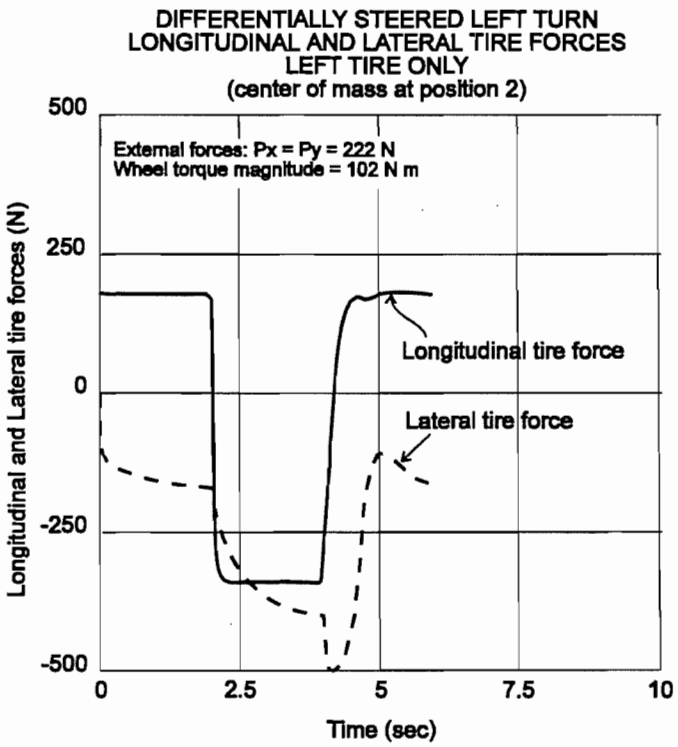

FIGURE 6-9
Left tire forces - Torque controlled turn - 102 N-m (75 ft-lbf).

The TMR path trace and left tire forces for the simulation with the applied wheel torque magnitude of 204 N-m (150 ft-lbf) are shown in Figures 6-10 and 6-11 respectively. Clearly in this simulation, the traction limits have been exceeded. From Figure 6-11, the tradeoff between the longitudinal and lateral tire forces can be seen from t = 2 to 4 seconds. As the TMR is turning, the need for lateral tire force increases, which, because the tire limits have been exceeded, causes a decrease in the longitudinal tire force. This indicates that there is excessive longitudinal and lateral slippage occurring. This accounts for the large error now associated with the dynamic (without tire) model shown in Figure 6-10.

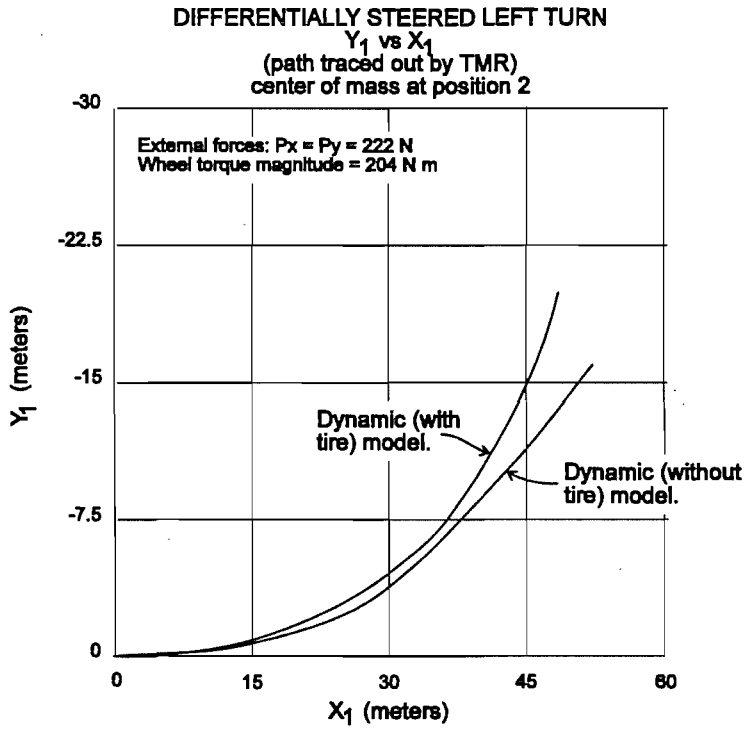

FIGURE 6-10
TMR path trace - Torque controlled turn - 204 N-m (150 ft-lbf)

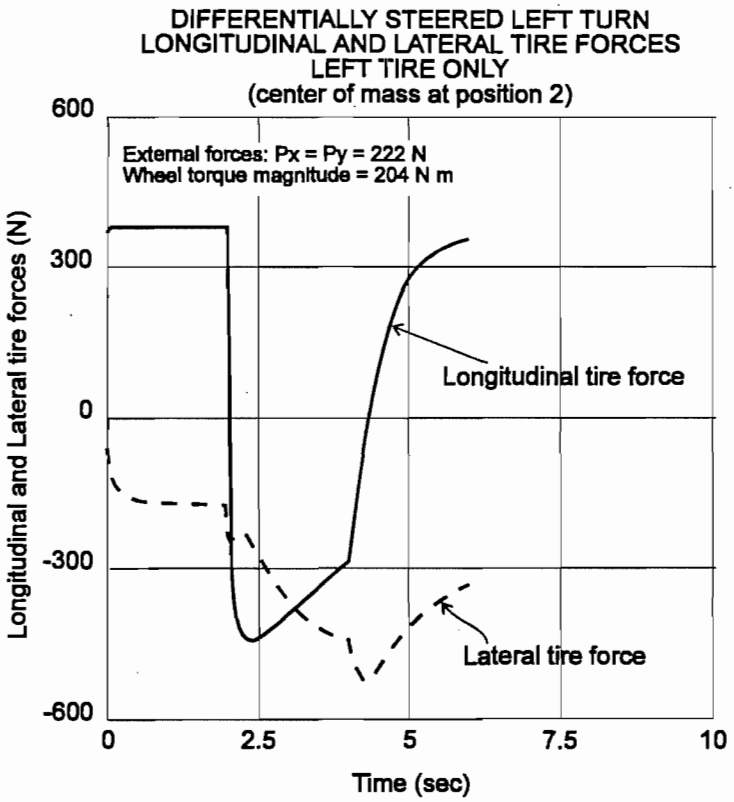

FIGURE 6-11
Left tire forces - Torque controlled turn - 204 N-m (150 ft-lbf).

CHAPTER 7. DYNAMICS OF CONVENTIONALLY STEERED WHEELED MOBILE ROBOTS

Similar to the format of Chapter 6, the dynamic equations for conventionally steered WMR's are derived in this chapter. The three conventionally steered TMR models will then be compared to one another through the use of simulation to find the limits of accuracy of each model.

7-1. Derivation of Dynamic Equations.

For the conventionally steered Tethered Mobile Robot is shown in Figure 2-2, the force and moment equations can easily be summed by inspection yielding

$$\sum F_x = m(\dot{u} - vr) = F_{xrl} + F_{xrr} + F_{xf}\cos\delta - F_{yf}\sin\delta + P_x \tag{7-1}$$

$$\sum F_y = m(\dot{v} + ur) = F_{yrl} + F_{yrr} + F_{yf}\cos\delta + F_{xf}\sin\delta + P_y \tag{7-2}$$

$$\sum M_z = I_z\dot{r} = \frac{T_r}{2}(F_{xrl} - F_{xrr}) - b(F_{yrl} + F_{yrr}) + a(F_{yf}\cos\delta + F_{xf}\sin\delta) - dP_y. \tag{7-3}$$

Solving the three equations for the longitudinal, lateral, and yaw accelerations, $\dot{u}$, $\dot{v}$, and $\dot{r}$ respectively, yields

$$\dot{u} = \frac{F_{xrl} + F_{xrr} + F_{xf}\cos\delta - F_{yf}\sin\delta + P_x}{m} + vr \tag{7-4}$$

$$\dot{v} = \frac{F_{yrl} + F_{yrr} + F_{yf}\cos\delta + F_{xf}\sin\delta + P_y}{m} - ur \tag{7-5}$$

$$\dot{r} = \frac{\frac{T_r}{2}(F_{xrl} - F_{xrr}) - b(F_{yrl} + F_{yrr}) + a(F_{yf}\cos\delta + F_{xf}\sin\delta) - dP_y}{I_z}. \tag{7-6}$$

Just as in Chapter 6, the three state variables, the longitudinal, lateral, and yaw velocities (u, v, r), are simply the integral of their accelerations

$$u = \int \dot{u}\, dt \qquad \textit{(longitudinal velocity)} \tag{6-7}$$

$$v = \int \dot{v}\, dt \qquad \textit{(lateral velocity)} \tag{6-8}$$

$$r = \int \dot{r}\, dt \qquad \textit{(yaw velocity)} \tag{6-9}$$

and the orientation of the vehicle with respect to the world coordinate system (yaw angle) is then determined by taking the integral of the yaw velocity

$$\psi = \int r\, dt. \tag{6-10}$$

With the forward, lateral, and yaw velocities along with the yaw angle, the equations for velocity and position of the TMR in the world coordinate system are identical to those of the kinematic model at the end of Chapter 3:

In the world coordinate system, the velocity of the linkage connection point $\mathbf{V_o}$ of the TMR is

$$\mathbf{V_o} = U\hat{i}_1 + V\hat{j}_1 \tag{3-12}$$

$$U = u\cos(\psi) - v\sin(\psi) - er\sin(\psi) \tag{3-13}$$

$$V = u\sin(\psi) + v\cos(\psi) + er\cos(\psi) \tag{3-14}$$

and the position of the linkage connection point $\mathbf{R_o}$ in the world coordinate system is

$$\mathbf{R_o} = X_1\hat{i}_1 + Y_1\hat{j}_1 \tag{3-15}$$

$$X_1 = \int U\, dt \tag{3-16}$$

$$Y_1 = \int V\, dt. \tag{3-17}$$

TIRE FORCES

Once again the Dugoff tire friction model is used to predict the forces produced by the tires. The rear tire forces are determined exactly the way they were determined in Chapter 6 for the differentially steered vehicle:

The normal force supported by each of the rear left and right wheels is written as

$$F_{N(left)} = F_{N(right)} = (\frac{mg}{2})\frac{a}{a+b} \tag{6-12}$$

and the load supported by the front steered wheel is

$$F_{N(front)} = mg\frac{b}{a+b}. \tag{6-20}$$

The longitudinal and lateral velocities of the right rear wheel are

$$V_{rtx} = u - r\frac{T_r}{2} \qquad \textit{(longitudinal velocity)} \tag{6-13}$$

$$V_{rty} = v - rb \qquad \textit{(lateral velocity)} \tag{6-14}$$

and similarly for the left rear wheel:

$$V_{ltx} = u + r\frac{T_r}{2} \qquad \textit{(longitudinal velocity)} \tag{6-15}$$

$$V_{lty} = v - rb \qquad \textit{(lateral velocity).} \tag{6-16}$$

In order to find the front tire forces, the longitudinal and lateral components of the front wheel velocity need to be found. The velocity of the steered front wheel with respect to the wheel orientation (tire fixed reference frame) was derived in Section 4-3 and is expressed as

$$\mathbf{V}_f = [u\cos\delta + (v+ar)\sin\delta]\hat{i}_3 + [(v+ar)\cos\delta - u\sin\delta]\hat{j}_3 \tag{4-38}$$

so the longitudinal and lateral components of the front wheel velocity V_{fx} and V_{fy} with respect to the wheel orientation are written as

$$V_{fx} = u\cos\delta + (v + ar)\sin\delta \tag{7-7}$$

$$V_{fy} = (v + ar)\cos\delta - u\sin\delta. \tag{7-8}$$

The wheel angular velocities can once again be determined in two ways: They can be specified if this dynamic model is being compared to the kinematic model, or in any other situation, the wheel speeds would need to be calculated by the following equations as were derived in Chapter 6.

The wheel angular acceleration $\dot{\omega}$ is written as

$$\dot{\omega} = \frac{N - F_{xt}R_t}{I_t} \tag{6-18}$$

and wheel speed ω is the integral of the wheel angular acceleration

$$\omega = \int \dot{\omega}\, dt. \tag{6-19}$$

These wheel angular velocity relations are valid for any wheel by using the applied torque, longitudinal tire force, tire radius, and moment of inertia all of which correspond to the tire of interest.

7-2. SIMULATION AND RESULTS

7-2-1. Comparison of dynamic and kinematic conventionally steered models with controlled wheel speeds.

To demonstrate the importance of the dynamic model, it was compared to the kinematic model. To compare these two models, both were run through identical situations to perform a simple maneuver. This maneuver was a simple 90 degree left hand turn similar in nature to a turn that a conventionally steered TMR would be expected to perform. Because the kinematic model is used in the comparison, one wheel speed along with the steering angle must be specified as functions of time. As was derived in Chapter 3 for the TMR, the specified wheel speed is the right rear wheel. The wheel speed form of the Dynamic model was used accordingly.

The same vehicle dimensions and parameters as with the differentially steered TMR simulation are used here with the addition of the front wheel moment of inertia:

TMR mass = 272 kg (18.6 slugs).
Tire radius = 0.3048 m (1.0 ft).
Longitudinal tire stiffness (all tires) = 40034 N/rad (9000 lbf/rad)
Lateral tire stiffness (all tires)= 40034 N/rad (9000 lbf/unit slip)
Road/tire interface coefficient of friction = 0.8
Yaw moment of inertia = 407 kg m^2 (300 ft lb sec^2)
Front wheel moment of inertia = 2.71 kg m^2 (2 ft lb sec^2)
Combined rear wheel, gearbox, and motor rotor moments of inertia
= 6.78 kg m^2
(5 ft lb sec^2)

Vehicle dimensions:

a = 0.762 m (2.5 ft).
b = 0.6096 m (2.0 ft).
d = 0.9144 m (3.0 ft).
e = 0.2286 m (0.75 ft).
T_r = 0.9144 m (3.0 ft).

The complete maneuver was accomplished as follows:

- The TMR was initially located at point (0,0) with an orientation of $\phi = 0$ degrees in the world coordinate system with an initial velocity in the $\hat{i}_1$ direction corresponding to the right wheel angular velocity (ω_r). The steered angle is zero ($\alpha = 0$ degs). The right wheel angular velocity ω_r is held constant throughout the maneuver.
- At a certain point in time, the front wheel is steered to a maximum angle of -30 degrees (a negative steering angle causes a left hand turn) as a quarter sine wave. The steered angle is held at -30 degrees for a period of time, and then steered back to zero degrees also as a quarter sine wave. The rate at which the front wheel is steered is dependent on the velocity of the TMR. A graph of the steered angle is shown in Figure 7-1.

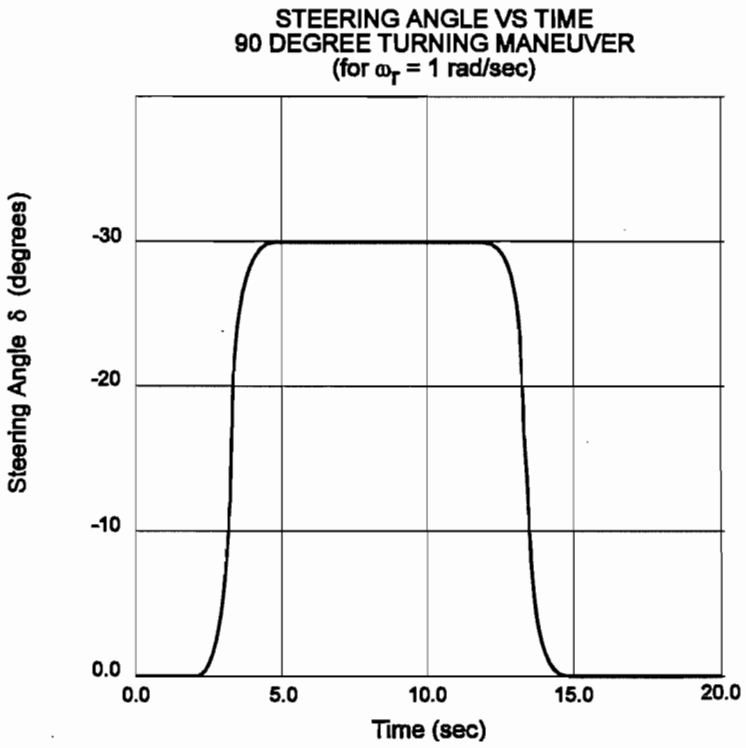

FIGURE 7-1
Front wheel steering angle as a function of time for $\omega_r = 1$ rad/sec

Figure 7-1 is for ω_r = 1 rad/sec and will vary depending on the value of ω_r (although the basic shape will remain the same and the maximum steered angle is always -30 degrees). After the turning maneuver, the TMR is allowed to travel in a straight line for a few moments to illustrate the difference in predicted paths between the models. The total time simulated varies depending on the speed that the TMR is simulated at (to produce comparable results).

- The maneuver is run at four different vehicle speeds: 0.3048 m/s (1 ft/s), 0.9144 m/s (3 ft/s), 1.524 m/s (5 ft/s), and 3.048 m/s (10 ft/s).

In order to keep the results simple, it is assumed that there are no router forces being exerted on the vehicle:

$$P_x = P_y = 0$$

The path traced out by the TMR is shown in Figure 7-2 for the four different simulated speeds.

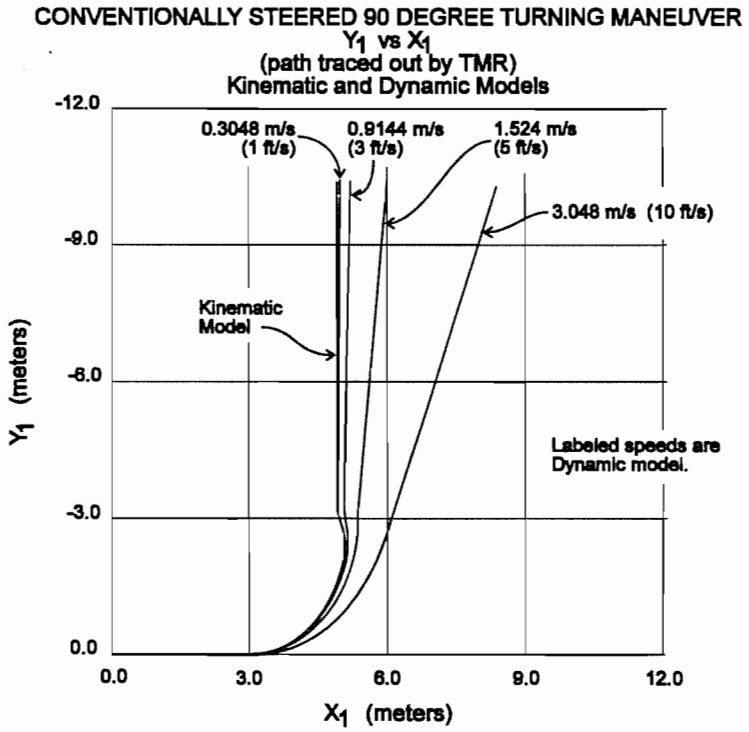

FIGURE 7-2
TMR path trace - 90 Degree turn simulation results

Figure 7-2 shows that the designated conventionally steered turn (radius of curvature ~2.5 m (~8 ft)) is not nearly as tight as that of the differentially steered turn. Conventionally steered vehicles are not designed to be as maneuverable as differentially steered vehicles. This turning maneuver is already an extremely sharp turn for a conventionally steered vehicle, and it would take an unrealistically large steering angle to approach the turning radius as was simulated by the differentially steered vehicle.

Once again, the kinematic model results are independent of vehicle speed, and will always predict a perfect 90 degree turn. The results from the dynamic model are quite different and highly dependent on vehicle speed. At a vehicle speed of about 0.3048 m/s (1 ft/s) or less, the predicted results of the dynamic model are nearly identical to that of the kinematic model. At a vehicle speed of 0.9144 m/s (3 ft/s) the differences are significant, and at any higher speeds, the differences become drastic.

According to these results, a conventionally steered wheeled mobile robot simulation using dead reckoning navigation techniques, traveling at a velocity of 1.524 m/s (5 ft/s) will have a location error of slightly over 1 meter (3 ft), only 10 meters (33 ft) after making the turning maneuver.

7-2-2. Comparison of Dead Reckoning method, Dynamic (with tire), and Dynamic (without tire) conventionally steered models with controlled wheel torques.

In this section the importance of the tire model for conventionally steered WMR's is demonstrated by comparing the dynamic (with tire) model to the dynamic (without tire) model. The dead reckoning predicted path is also shown in order to demonstrate the error associated with tracking the path of a real vehicle using the dead reckoning process.

For this simulation, the front wheel steering angle is specified as a function of time, and the applied rear wheel torques are specified. Equal torques are applied to both right and left rear wheels simulating a single motor which transfers power to the two driving wheels through the use of a differential (a standard differential provides equal torques to each driving wheel).

The simulated maneuver for this comparison is again, a left hand turn. Just as in Section 6-2-2, since the wheel torques are specified, the degree of attempted turn is not predetermined. The left turn is accomplished as follows:

- The TMR starts initially at point (0,0) with an orientation of $\psi = 0$ degrees in the world coordinate system with an initial velocity if 0.3048 m/sec (1 ft/sec) in the $\hat{i}_1$ direction with a steered angle of zero ($\alpha = 0$ degs). Both the right and left wheels are spinning accordingly. Equal and constant torques are applied to the right and left driving wheels. Three different torques are used in this simulation: 13.6 N-m (10 ft-lbf), 27.2 N-m (20 ft-lbf), and 40.8 N-m (30 ft-lbf).
- From time t = 2 seconds until time t = 4 seconds, the front wheel is steered to a maximum angle of -10 degrees (a negative steering angle causes a left hand turn) as a quarter sine wave in the same manner as was done in Section 7-2-1. The steered angle is held at -10 degrees for 2 seconds (from time t = 4 seconds until t = 6 seconds) and then steered back to zero degrees over a period of 2 seconds (from time t = 6 seconds until t = 8 seconds) as a function of a quarter sine wave. The vehicle is then allowed to

travel with a steering angle of zero degrees for an additional 2 seconds. The total time simulated for each situation is identical (10 seconds).

As in the previous simulation, it is assumed that there are no router forces being exerted on the vehicle:

$$P_x = P_y = 0.$$

The vehicle parameters outlined in Section 7-2-1 are also used in this set of simulations. The position of the center of mass is not varied as it was in the simulation of the differentially steered WMR in Section 6-2-2.

The results of the simulation showing the path traced out by the TMR for the three different applied wheel torques are shown in Figures 7-3 to 7-5. Each figure shows the predicted path for the dynamic (with tire) model, the dynamic (without tire) model, and the dead reckoning method.

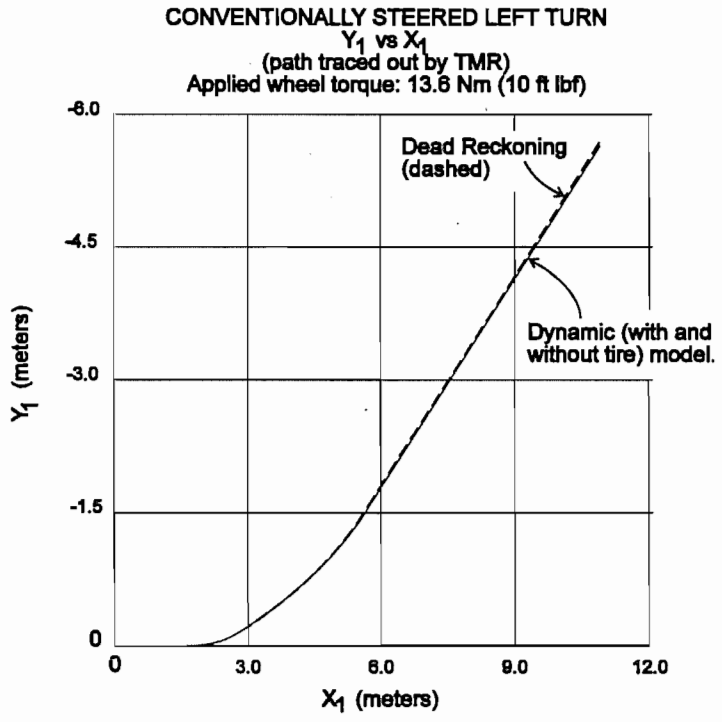

FIGURE 7-3
Conventionally steered TMR path trace - Applied wheel torque: 13.8 N-m (10 ft-lbf)

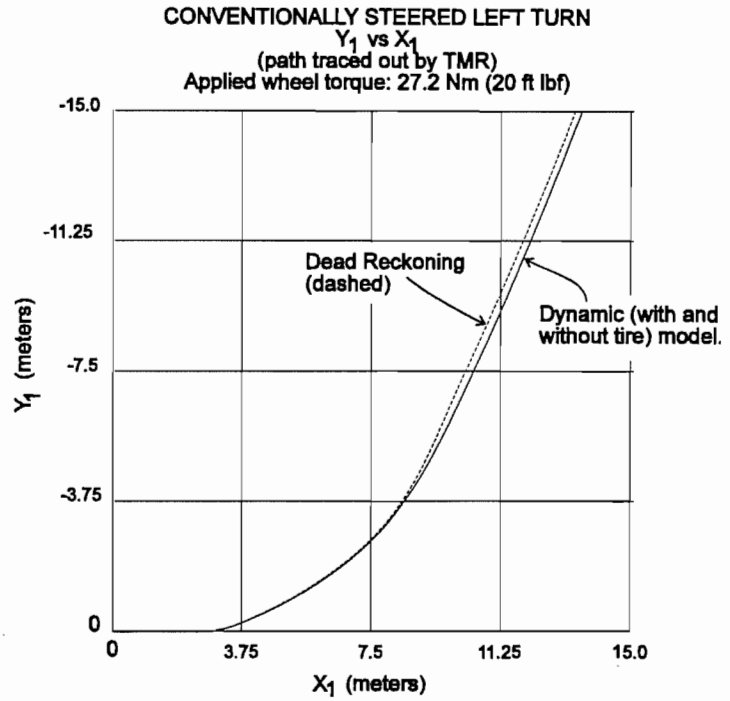

FIGURE 7-4
Conventionally steered TMR path trace - Applied wheel torque: 27.2 N-m (20 ft-lbf)

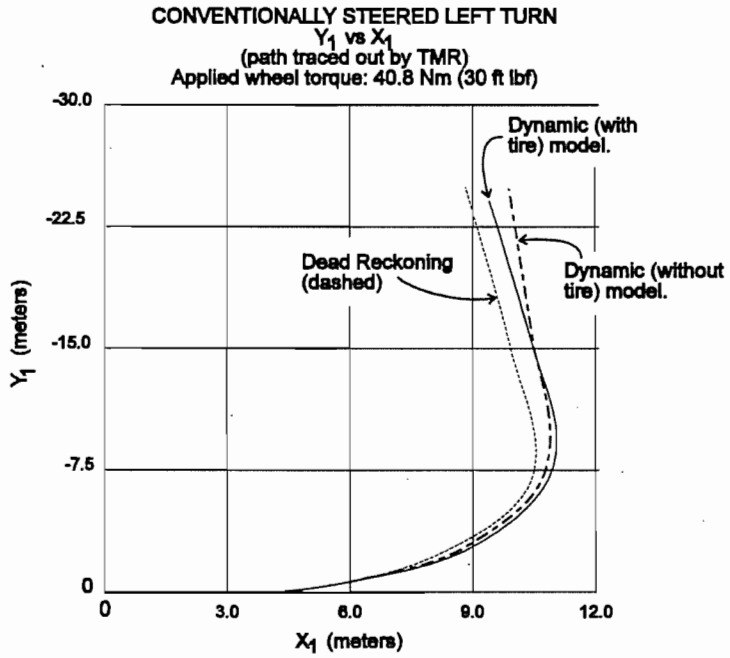

FIGURE 7-5
Conventionally steered TMR path trace - Applied wheel torque: 40.8 N-m (30 ft-lbf)

The different wheel torque magnitudes applied to the different simulations have two effects: 1. The higher applied wheel torque increases the longitudinal tire forces on the rear driving wheels, and 2. The greater the applied wheel torque, the greater the vehicle acceleration, which causes the vehicle to travel at a higher rate of speed when the maneuver takes place. For these simulations, the speed range at which the maneuvers took place are as follows:

Applied Wheel Torque	Vehicle Velocity Range
13.8 N-m (10 ft-lbf)	0.6 - 1.8 m/sec (2 - 6 ft/sec)
27.2 N-m (20 ft-lbf)	1.2 - 3.4 m/sec (4 - 11 ft/sec)
40.8 N-m (30 ft-lbf)	1.5 - 4.9 m/sec (5 - 16 ft/sec)

Figure 7-3 shows that both the dynamic models and the dead reckoning method are nearly identical for this low speed, low torque simulation. As the vehicle speed and torque are increased as in Figure 7-4, the dead reckoning method begins to vary noticeably from both of the dynamic models - which are still in agreement in this simulation. However, the dead reckoning method is still relatively accurate, only deviating from the dynamic models by not more than about 0.15 m (0.5 ft) after traveling a distance of approximately 18 m (60 ft). Large deviations from the dynamic (with tire) model, however, do show up in Figure 7-5 when the wheel torques are increased to 40.8 N-m (30 ft-lbf). Both the dead reckoning technique and the dynamic (no tire) model differ equally from the dynamic (with tire) model. The error associated with the dynamic (no tire) model and the dead reckoning method is about 0.6 m (2 ft) after traveling a distance of approximately 20 m (65 ft). For this particular situation, if the simulation was allowed to continue for a few more seconds, the dynamic (no tire) model would differ significantly more from the dynamic (with tire) model than would the dead reckoning results due to the difference in yaw angle predicted by the dynamic (no tire) model.

In order to find the general limits of validity of the different models, it is necessary to take a look at the tire forces involved in these simulations. Figures 7-6 and 7-7 show the right rear and the front tire forces respectively (right rear tire forces are shown because they are greater than the left rear tire forces) which correspond to the simulation results shown in Figure 7-4 (27.2 N-m (20 ft-lbf) wheel torque simulation).

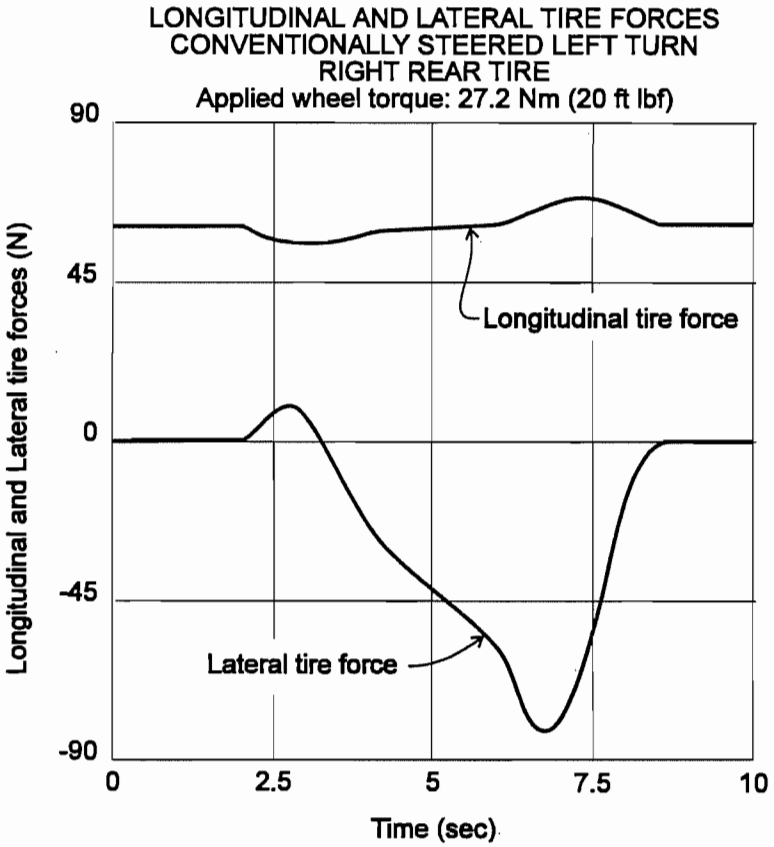

FIGURE 7-6
Right rear tire forces - Applied wheel torque: 27.2 N-m (20 ft-lbf)

From Figure 7-6, the maximum right rear tire forces occur somewhere around time t = 7 seconds, at which time the longitudinal and lateral tire forces are about 44.5 N (10 lbf) and -80 N (-18 lbf) respectively for a combined right rear tire force of approximately 93 N (21 lbf). From Figure 7-7, the maximum front tire forces occur at about time t = 6 seconds, at which time the longitudinal and lateral tire forces are about -11.5 N (-2.6 lbf)

and -130 N (-29 lbf) respectively for a combined front tire force of slightly more than 130 N (29 lbf).

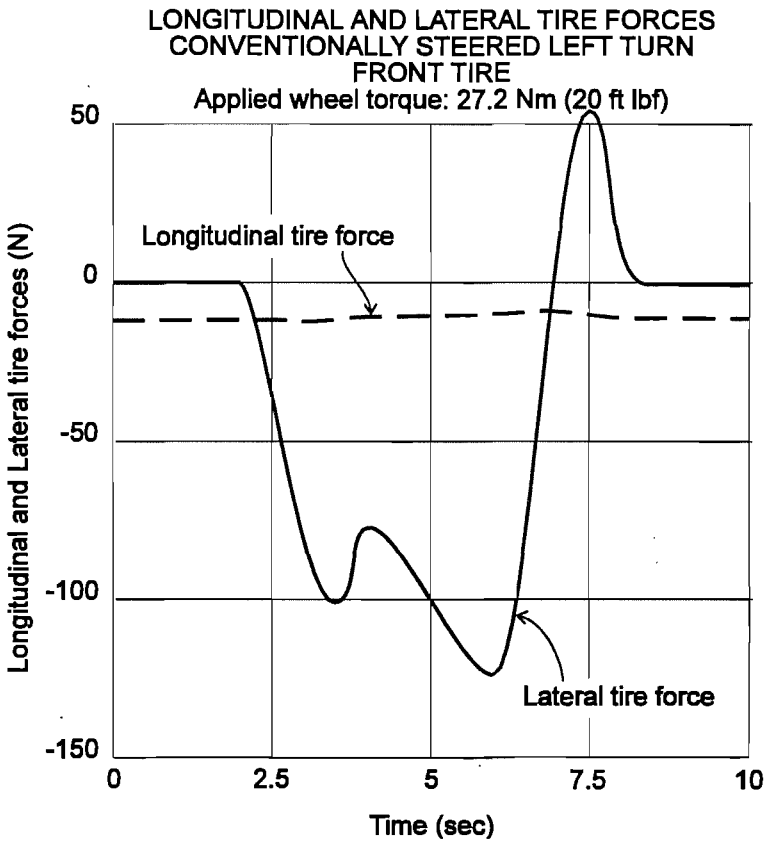

FIGURE 7-7
Front tire forces - Applied wheel torque: 27.2 N-m (20 ft-lbf)

For the conventionally steered TMR configuration and parameters, the right rear tire limits occur at about 600 N (135 lbf) and the front tire limits occur at about 930 N (210 lbf). This means that the right rear tire is operating at about 16% of its available force limits and the front tire is operating at about 14% of its available force limits. Both are well within the generally accepted range of validity of the dead reckoning kinematic tracking method, however, noticeable deviations in path prediction between the models is beginning to occur and be significant.

The tire forces for the right rear and front tires which correspond to the simulation results shown in Figure 7-5 (40.8 N-m (30 ft-lbf) wheel torque simulation) are shown in Figures 7-8 and 7-9 respectively.

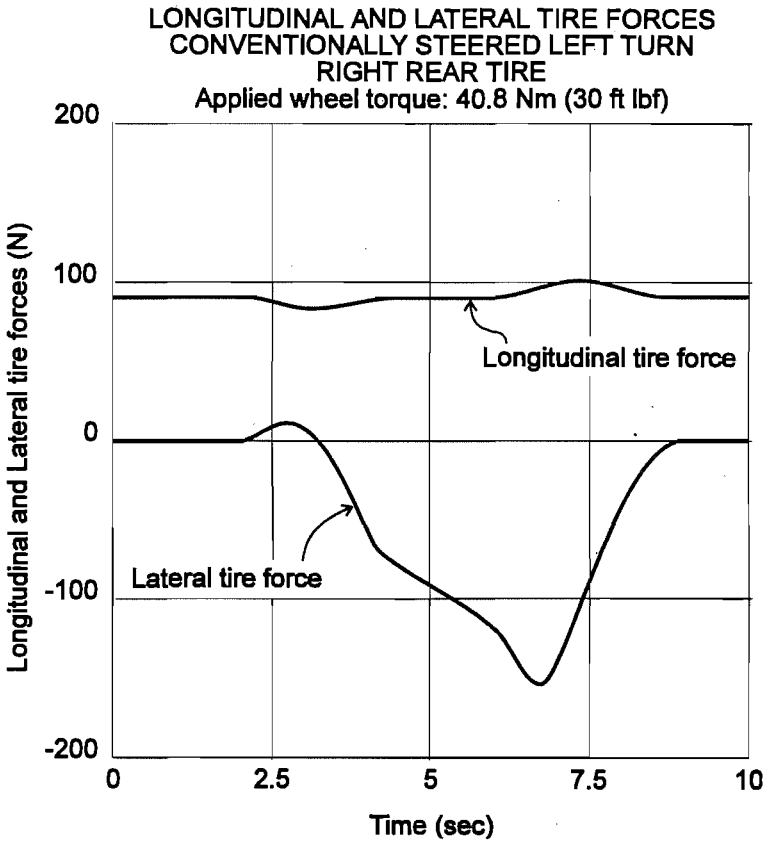

FIGURE 7-8
Right rear tire forces - Applied wheel torque: 40.8 N-m (30 ft-lbf)

From Figure 7-8, the maximum right rear tire forces occur somewhere around time t = 7 seconds, at which time the longitudinal and lateral tire forces are about 100 N (22 lbf) and -150 N (-34 lbf) respectively for a combined right rear tire force of approximately 180 N (40 lbf). From Figure 7-9, the maximum front tire forces occur at about time t = 6 seconds, at which time the longitudinal and lateral tire forces are about -16 N (-3.5 lbf) and -250 N (-56 lbf) respectively for a combined front tire force of slightly more than 250 N (56 lbf).

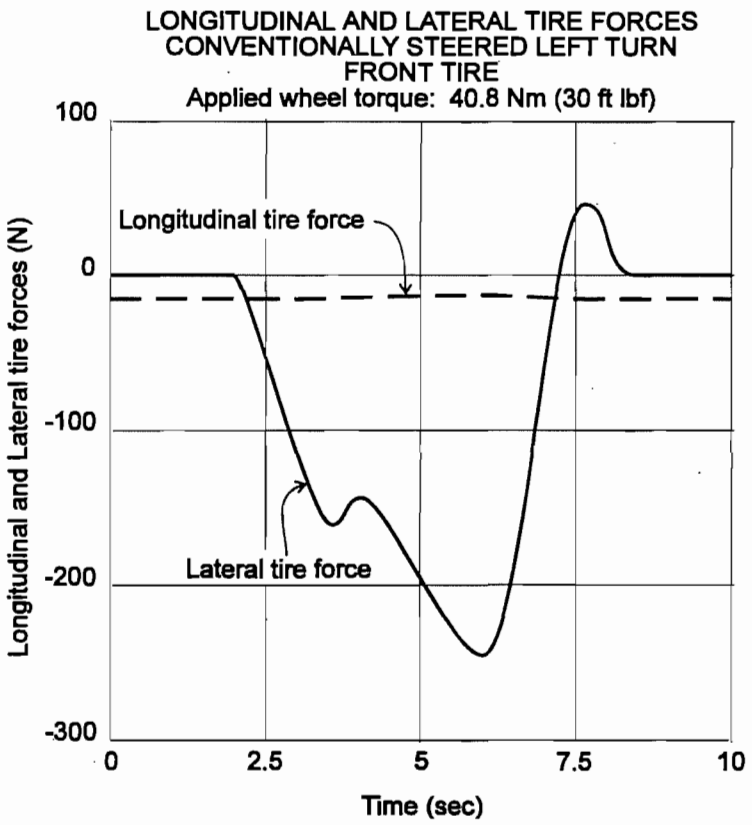

FIGURE 7-9
Front tire forces - Applied wheel torque: 40.8 N-m (30 ft-lbf)

As was stated before, the right rear tire limits occur at about 600 N (135 lbf) and the front tire limits occur at about 930 N (210 lbf). This means that the right rear tire is operating at about 30% of its available force limits and the front tire is operating at about 27% of its available force limits. Although the generated tire forces are getting large, they are still well within the limits of the tires and within the generally accepted range of validity of the dead reckoning kinematic tracking method. However, the path trace from Figure 7-5 shows that neither the dead reckoning method nor the dynamic (no tire) model are even reasonably accurate and should by no means be used to predict the position and orientation of a wheeled mobile robot under these conditions.

CHAPTER 8. CONCLUSIONS AND RECOMMENDATIONS

The purpose of this paper was to show the importance and significance of dynamic modeling of wheeled mobile robots. The kinematic model, which is the method most researchers have used to track WMR's, was compared to a dynamic model through computer simulation. The advantage of the kinematic model is its simplicity, but this is also where its shortcomings lie. For simulation purposes, masses and moments of inertia, along with external forces and torques do not affect the velocity, position, or orientation of the WMR in any way. For both differentially and conventionally steered WMR's, it was found that a kinematic model cannot accurately predict the position and orientation of a 'working' WMR under almost any conditions. Use of the kinematic model must be limited to lightweight vehicles which operate under very low speeds, very low accelerations, and under lightly loaded conditions. An additional drawback to the kinematic model for use in simulation purposes is the fact that wheel speeds must be the specified variables, whereas in a real vehicle, wheel speeds cannot realistically be specified. From these results it is concluded that dynamic modeling of any 'working' WMR is extremely important due to the fact that a kinematic representation fails to provide reasonable accuracy under common working and maneuvering conditions.

The kinematic model is also used to track the position of real vehicles by measuring wheel speeds directly, a process called dead reckoning. It has been shown that for both differentially and conventionally steered WMR's the potential error associated with this method is large, even when the tires are producing forces at only a fraction of their friction potential, where dead reckoning is generally assumed to be relatively accurate. This demonstrates that vehicle tracking through the use of dead reckoning for a WMR when wheel speeds are measured off of the driving wheels is much less accurate than commonly thought. Once again, dead reckoning is only valid on small, lightweight

vehicles which operate under very low speeds, very low accelerations, and under lightly loaded conditions.

Another aspect of this work was to determine the importance of using a complex tire representation when dynamically modeling a WMR. A dynamic model without a tire model was created to investigate this. For differentially steered vehicles, this dynamic (without tire) model was surprisingly accurate, even approaching the friction limits of the tires. A complete and accurate tire model (such as the Dugoff tire model) is irreplaceable for any complete dynamic model which may encounter situations where the tire limits are approached or reached. However, for a differentially steered WMR which is known to stay well within the traction limits of the tires, very simple tire models can be used (or no tire model as was derived in this paper) with excellent accuracy. A good rule of thumb for differentially steered WMR's is probably this: If the WMR is known to stay within 50% of the tire traction limits, simple tire models (or no tire model) provide excellent accuracy and can be used with confidence; If the WMR is expected to exceed 50% of the traction limits, a more accurate tire model (one which incorporates the friction circle concept) is in order to ensure accurate simulation results.

For conventionally steered vehicles, the dynamic (without tire) model was only accurate to a fraction of the tire friction limits. In fact, the dynamic (without tire) model had an accuracy range similar to that of the dead reckoning method. Because the limits of accuracy for conventionally steered WMR's were found to be at such low tire friction levels, it is suggested that dynamic modeling incorporating the use of an accurate tire model should always be used when simulating conventionally steered wheeled mobile robots.

It is important to note that only 3 degree of freedom dynamic models were used in this paper in order to keep the results straightforward to interpret. As degrees of freedom are added to the dynamic model, (roll, pitch, bounce, weight transfer, etc), the accuracy of

the dynamic model will increase, although further discrepancies from other models are expected to be small in comparison to those demonstrated here.

While this work has contributed to the understanding of the importance of dynamic modeling of differentially and conventionally steered wheeled mobile robots, there remains room to extend this work and provide additional contributions. Throughout this work, a three degree of freedom dynamic model was used. Extending this to include additional degrees of freedom such as roll, pitch, bounce, weight transfer, etc., will increase the accuracy of the model.

Another extension of this work is the investigation of the accuracy of the dead reckoning method of vehicle tracking when using passive wheels (both rigidly mounted and caster-type wheels) instead of driven wheels. This method is expected to be significantly more accurate than the driven wheel dead reckoning method which was investigated here, but the degree of accuracy is yet unknown.

Finally, this work investigated the dynamic modeling of wheeled mobile robots with conventional wheels. While conventional wheels are most common at this time, much research is now being devoted toward the development of omnidirectional type wheels and wheeled mobile robots which make use of these types of wheels. Although the dynamic modeling of omnidirectional WMR's is significantly more complex than that of conventionally wheeled WMR's, it is a logical extension of this work as we advance toward the future of wheeled mobile robots.

REFERENCES

Alexander, J.C. and Maddocks, J.H., 1989, "On the Kinematics of Wheeled Mobile Robots", The International Journal of Robotics Research, Vol. 8, No. 5, pp 15-27.

Campion, G., Bastin, G. and Andréa-Novel, B.D., 1993, "Structural Properties and Classification of Kinematic and Dynamic Models of Wheeled Mobile Robots", 1993 IEEE International Conference on Robotics and Automation, Vol 1, pp 462-469.

Dugoff, H., Fancher, P.S. and Segal, L., 1970, "An Analysis of Tire Traction Properties and Their Influence on Vehicle Dynamic Performance", Paper No. 700377, SAE Transactions, pp. 1219-1243.

Gentile, A. and Luigi, M., 1992, "Comparisons Between Different Mobile Robot Configurations", Proceedings of the 3rd International Workshop on Advances in Robot Kinematics, Ferrara, Italy.

Gillespie, T.D., 1992, "Fundamentals of Vehicle Dynamics", Society of Automotive Engineers, Inc., Pennsylvania.

Guntur, R. and Sankar, S., 1980, "A friction circle concept for Dugoff's tyre friction model", International Journal of Vehicle Design, Vol. 1, No. 4, pp 373-377.

Hamdy, A. and Badreddin, E., 1992, "Dynamic Modelling of a Wheeled Mobile Robot for Identification, Navigation, and Control", Robotics and Flexible Manufacturing Systems, Elsevier Science Publisher B. V. (North-Holland), pp. 119-128.

Hemami, A., Mehrabi, M.G. and Cheng, R.M.H., 1990, "A New Control Strategy for Tracking in Mobile Robots and AGV's", IEEE, pp. 1122-1127.

Segovia, A., Rombaut, M., Preciado, A. and Meizel, D., 1991, "Comparative Study of the Different Methods of Path Generation for a Mobile Robot in a Free Environment", 1991 IEEE Conference, pp. 1667-1670.

Smith, D. E., Starkey, J. M., 1991, "Overview of Vehicle Models, Dynamics, and Control Applied to Automated Vehicles." In Velinsky, S. A., Fries, R. H., and Wang, D., editors, Winter Annual Meeting of the ASME, pp. 69-87.

Winters, S. E., 1992, "Development of a Tethered Mobile Robot", University of California, Masters Thesis.

Winters, S. E., Hong, D., Velinsky, S. A., and Yamazaki, K., 1994, "A New Robotic System Concept for Automating Highway Maintenance Tasks", Proceedings of the ASCE Conference on Robotics for Challenging Environments, to appear.

APPENDIX

Derivation of the Rigid Body Equations of motion with respect to a Body Centered Frame of Reference.

The standard body centered reference frame (SAE vehicle axis system) of a vehicle is depicted in Figure A-1:

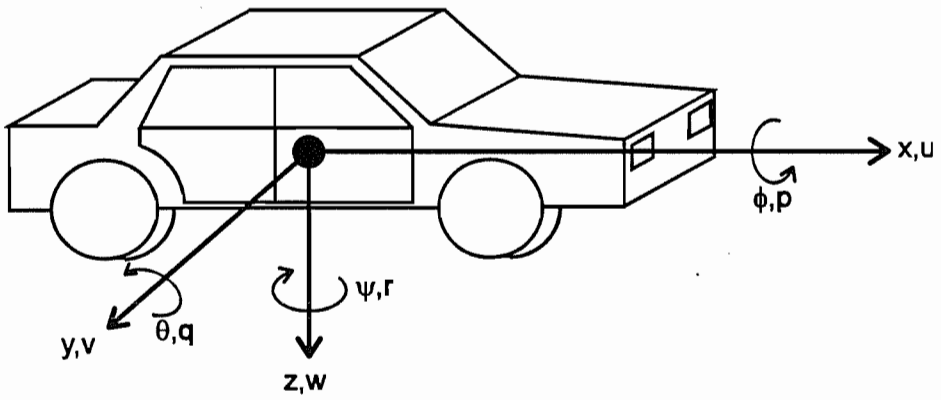

FIGURE A-1
Body Centered Reference Frame

Direction	x	y	z
Linear Velocity	u	v	w
Angular Displacement	ϕ	θ	ψ
Angular Velocity	p	q	r

The body centered reference frame (xyz) is a rotating coordinate system. To derive the rigid body equations of motion with respect to this system, it is necessary to make use of an absolute coordinate system, which will be referred to as the inertial reference frame (XYZ). The body centered reference frame rotates within the inertial reference frame at

the same angular velocity as the vehicle angular velocity ω given by the following expression

$$\boldsymbol{\omega} = p\hat{i} + q\hat{j} + r\hat{k} \tag{A-1}$$

where p, q, and r, are the roll, pitch, and yaw angular velocities.

The vehicle linear velocity **v** is expressed as

$$\mathbf{v} = u\hat{i} + v\hat{j} + w\hat{k} \tag{A-2}$$

where u, v, and w are the forward, lateral, and vertical velocities.

The sum of Forces equals the time rate of change of linear momentum (in the inertial reference frame (XYZ)):

$$\sum \mathbf{F} = \left.\frac{d(m\mathbf{v})}{dt}\right|_{XYZ} = m\left.\frac{d\mathbf{v}}{dt}\right|_{XYZ} \qquad \textit{(for m=constant)} \tag{A-3}$$

and the sum of moments equals the time rate of change of moment of momentum (in the inertial reference frame (XYZ))

$$\sum \mathbf{M} = \left.\frac{d(\mathbf{H})}{dt}\right|_{XYZ}. \tag{A-4}$$

It is easiest to take the derivative of the velocity with respect to the body fixed reference frame (xyz)

$$\begin{aligned} \left.\frac{d\mathbf{v}}{dt}\right|_{XYZ} &= \left.\frac{d\mathbf{v}}{dt}\right|_{xyz} + (\boldsymbol{\omega} \times \mathbf{v}) \\ &= (\dot{u} + qw - vr)\hat{i} + (\dot{v} + ur - pw)\hat{j} + (\dot{w} + pu - qu)\hat{k} \end{aligned} \tag{A-5}$$

so the sum of the forces with respect to the body fixed reference frame (xyz) in each of its three principal directions can now be written independently as

$$\sum F_x = m(\dot{u} + qw - vr) \tag{A-6}$$
$$\sum F_y = m(\dot{v} + ur - pw) \tag{A-7}$$
$$\sum F_z = m(\dot{w} + pu - qu). \tag{A-8}$$

For the moment equation (A-4)

$$\left.\frac{d\mathbf{H}}{dt}\right|_{XYZ} = \left.\frac{d\mathbf{H}}{dt}\right|_{xyz} + (\omega \times \mathbf{H}). \tag{A-9}$$

In general, the moment of momentum of rigid body 'B' about some point P is written:

$$\mathbf{H} = \int_m (\mathbf{r} \times [\omega \times \mathbf{r}])dm \tag{A-10}$$

where **r** is the position vector from point P to a point mass Q in the body B

$$\mathbf{r} = x\hat{i} + y\hat{j} + z\hat{k}. \tag{A-11}$$

Crossing ω into **r** gives

$$\omega \times \mathbf{r} = (qz - ry)\hat{i} + (rx - pz)\hat{j} + (py - qx)\hat{k} \tag{A-12}$$

and then crossing **r** into [ω x **r**] yields

$$\begin{aligned}(\mathbf{r} \times [\omega \times \mathbf{r}]) = &[y(py - qx) - z(rx - pz)]\hat{i} \\ &+[z(qz - ry) - x(py - qx)]\hat{j} \\ &+[x(rx - pz) - y(qz - ry)]\hat{k}.\end{aligned} \tag{A-13}$$

The moment of momentum in the x direction only can be written as

$$\begin{aligned}H_x &= \int_m (y^2 p - xyq - zxr + z^2 p)dm \\ &= p\int_m (y^2 + z^2)dm - q\int_m (xy)dm - r\int_m (xz)dm.\end{aligned} \tag{A-14}$$

But, from the definition of the moment and product of inertias we have the following equations:

$$\int_m (y^2 + z^2)dm = I_x \qquad \textit{(moment of inertia of Body B about x)} \qquad \text{(A-15)}$$

$$\int_m (xy)dm = I_{xy} \qquad \textit{(product of inertia about x and y)} \qquad \text{(A-16)}$$

$$\int_m (xz)dm = I_{xz} \qquad \textit{(product of inertia about x and z).} \qquad \text{(A-17)}$$

Substituting in for the inertia expressions yields

$$H_x = I_x p - I_{xy} q - I_{xz} r. \qquad \text{(A-18)}$$

Similarly, the moment of momentum in the y and z directions yields

$$H_y = I_y q - I_{yz} r - I_{xy} p \qquad \text{(A-19)}$$

$$H_z = I_z r - I_{xz} p - I_{yz} q. \qquad \text{(A-20)}$$

Now, taking the derivative with respect to time of the moment of momentum produces

$$\left.\frac{d\mathbf{H}}{dt}\right|_{xyz} = (I_x \dot{p} - I_{xy}\dot{q} - I_{xz}\dot{r})\hat{i} + (I_y \dot{q} - I_{yz}\dot{r} - I_{xy}\dot{p})\hat{j} + (I_z \dot{r} - I_{xz}\dot{p} - I_{yz}\dot{q})\hat{k} \qquad \text{(A-21)}$$

and crossing ω into the moment of momentum gives

$$\begin{aligned}\omega \times \mathbf{H} = {} & [q(I_z r - I_{xz} p - I_{yz} q) - r(I_y q - I_{yz} r - I_{xy} p)]\hat{i} \\ & + [r(I_x p - I_{xy} q - I_{xz} r) - p(I_z r - I_{xz} p - I_{yz} q)]\hat{j} \\ & + [p(I_y q - I_{yz} r - I_{xy} p) - q(I_x p - I_{xy} q - I_{xz} r)]\hat{k}.\end{aligned} \qquad \text{(A-22)}$$

Adding (A-21) and (A-22) gives expressions for the moment equations WRT the body fixed reference frame (xyz) in the longitudinal, lateral, and vertical directions

$$\sum M_x = I_x \dot{p} - I_{xy}(\dot{q} - pr) - I_{xz}(\dot{r} + pq) + (I_z - I_y)qr + I_{yz}(r^2 - q^2) \qquad \text{(A-23)}$$

$$\sum M_y = I_y\dot{q} - I_{yz}(\dot{r} - pq) - I_{xy}(\dot{p} + qr) + (I_x - I_z)pr + I_{xz}(p^2 - r^2) \tag{A-24}$$

$$\sum M_z = I_z\dot{r} - I_{xz}(\dot{p} - qr) - I_{yz}(\dot{q} + pr) + (I_y - I_x)pq + I_{xy}(q^2 - p^2). \tag{A-25}$$

In most vehicles, including wheeled mobile robots, the xz plane can be approximated as a plane of symmetry, which causes the product of inertia about x and y to drop out

$$\Rightarrow I_{xy} = I_{yz} = 0$$

which simplifies equations (A-23), (A-24), and (A-25) to the following expressions:

$$\sum M_x = I_x\dot{p} - I_{xz}(\dot{r} + pq) + (I_z - I_y)qr \qquad \textit{(roll)} \tag{A-26}$$

$$\sum M_y = I_y\dot{q} + (I_x - I_z)pr + I_{xz}(p^2 - r^2) \qquad \textit{(pitch)} \tag{A-27}$$

$$\sum M_z = I_z\dot{r} - I_{xz}(\dot{p} - qr) + (I_y - I_x)pq \qquad \textit{(yaw).} \tag{A-28}$$